MASTERARBEIT | MASTER'S THESIS

Titel | Title

Functioncal Rescue Of Disease Variants In SLC6 Transporters

verfasst von | submitted by

Diksha Kunj BSc

angestrebter akademischer Grad | in partial fulfilment of the requirements for the degree of

Magistra pharmaciae (Mag. pharm.)

Wien | Vienna, 2025

Studienkennzahl lt. Studienblatt | Degree programme code as it appears on the student record sheet:	UA 066 605
Studienrichtung lt. Studienblatt | Degree programme as it appears on the student record sheet:	Masterstudium Pharmazie
Betreut von | Supervisor:	Sonja Sucic

Acknowledgments

First and foremost, I express my deepest gratitude to my supervisor Dr. Sonja Sucic, who has provided me with the greatest kind of mentoring throughout my journey. Her love for the project and excitement has kept me encouraged from week to week. The amount of respect I have gained for Dr. Sonja Sucic is unmeasurable and I am very thankful for her encouragement that has kept me going for the duration of the thesis. I learned a lot from her and am so proud that I was eligible to join her team.

The completion of this thesis would not have been possible either without the support of Shima, who has guided me from the beginning to the end with the experiments and supported me all the way. Without her I would not have come this far, on a scientific as well as on a personal level. I feel proud to have gained such a dear friend during my time.

I would love to send my gratitude to Nicholas Kirsch, who has provided me with a necessary illustration of the NET synthesis for my thesis, as he has put a lot of effort into it himself. I would also love to extend my gratitude towards my other colleagues Nikita and Catherine for their never-ending patience and support ever since the day I started in the lab. Even when I bombarded them with my questions, they kept answering them graciously and never got tired. I also want to thank my coworkers who kept me company and made the time more enjoyable. Thanks to them the lab was filled with a lot of laughter and joy. During my time not only have I gained a pool of knowledge, but along with those unforgettable memories and precious friendships.

Table of Content

Zusammenfassung

Neurotransmitter sind essentielle Figuren in der Signalweiterleitung, da diese primär die Information von Neuron zu Neuron induzieren. Insbesondere Noradrenalin und γ – Aminobuttersäure sind von großer Relevanz aufgrund ihrer unentbehrlichen Präsenz im Nervensystem. Damit allerdings die Neuronen nicht kontinuierlich aktiviert werden sollten, existieren sogenannte Wiederaufnahmetransporter, welche die Neurotransmitter zurück in die präsynaptische Nervenzelle aufnehmen und damit die Signalweiterleitung zum Halt bringen. Aus diesem Grund sind Transporter unabdinglich im Sinne der Modulation von Informationsübertragung und können allerdings bei Mutationen ein Spektrum von Krankheiten hervorbringen. Sobald einzelne Nukleotide im genetischen Code ausgetauscht werden, kann je nach Lokalisation der Mutation die Funktion des Transporters erheblich eingeschränkt werden. Diese Veränderung ist auf einen Fehler im Faltungsprozess des nativen Proteins zurückzuführen, welches im Nachhinein minimal bis kaum in der Zellmembran exprimiert wird. Eventuell wird die Wiederaufnahme von Noradrenalin und GABA reduziert oder im Ganzen eliminiert, sodass eine Spanne von Krankheiten daraus resultiert. Diese zieht sich von neurologischen Erkrankungen wie Epilepsie bis hin zu kardiovaskulären wie orthostatische Dysregulation.

In der Vergangenheit konnten erfolgreich so genannte Pharmakochaperonen und chemische Chaperonen an Mutationen dieser Art angewendet werden, welche die erneute Expression der Transporter ermöglichten. Mutierte Dopamin Transporter, welche aufgrund der fehlgefalteten Natur innerhalb der Zelle gefangen blieben, erlangten anhand dieser Methode ihre Funktionsfähigkeit zurück. Mithilfe von diesem Ansatz wollen wir mutierte Noradrenalin und GABA Transporter retten und ihre Expression wie auch Funktion wiederherstellen.

Abstract

Neurotransmission is the physiological pathway of communication that is provided by a variety of endogenous compounds, γ-aminobutyric acid (GABA) and norepinephrine (NE) setting essential examples, especially in the nervous system. Their respective transporters norepinephrine transporter (NET) and GABA transporter 1 (GAT1) modulate the neurotransmitter-mediated signalling by means of reuptake, in other words by taking up the neurotransmitter from the synaptic cleft and storing them in the presynaptic neuron until another impulse initiates a release. Consequently, neurotransmitter transporters play key roles in signal modulation – however, only if they work correctly. Single nucleotide polymorphisms (SNPs) have been brought in relation to impaired protein folding which eventually diminish the reuptake ability of the transporter. Depending on the site of mutation, the transporter might either show a decreased presence in plasma expression with reduced transport rate or be retained intracellularly and subsequently terminate any reuptake. Several variants of this kind are known for NET and GAT1 that are associated with a scale of disorders, spanning from neurological conditions like epilepsy and autism spectrum disorders to cardiovascular diseases such as orthostatic intolerance.

In hope to rescue the lost transporters and revive their functionality, we have employed a pool of small compounds as pharmacological and chemical chaperones. This group has demonstrated great efficacy in other loss-of-function proteins known for serotonin and dopamine transporters, latter severely presented in patients suffering from infantile Parkinson's disease or dopamine transporter deficiency syndrome (DTDS). As the approach of chaperoning has proven effects on these transporters before, we applied pharmacological and chemical chaperones on NET and GAT1 mutants in order to examine their potential effects on correcting the folding trajectories of misfolded mutants.

1 Introduction

Neuronal transmission occurs when neurons transmit information each other by utilizing an electrical gradient and chemically communicating with the neighbouring nerve cells. Once an electrical impulse moves along the axon and arrives at the presynaptic neuron, it triggers the release of vesicles packed with neurotransmitters into the synaptic cleft, where they act on either pre- or postsynaptic receptors (1). However, once in the synaptic cleft, the neurotransmitters need to be removed to achieve signal modulation. In this regard, the idea of neurotransmitter reuptake was first born in the early 1960s. The control over signal transmission is obtained by transporters which take up the neurotransmitter back into the neuron and subsequently cease overstimulation of postsynaptic neurons. The first transporter to be described with such function is NET, a member of the solute carrier 6 (SLC6) family (2). It paved the way to discover more members of the same family, such as the GABA transporters as well as monoamine transporters, and allowed to conduct experimental studies on the type of transport that is active for the SLC6 group. As of today, we know that this family belongs to the neurotransmitter-sodium-symporters (NSS), meaning that the substrate transport requires both Na^+ and Cl^- in order to eliminate the neurotransmitter from the extracellular compartment (3).

The SCL6 family is covered by 20 genes, encoding 4 subgroups, and plays an essential role in neurotransmitter clearance. Members of this group are well expressed in the nervous system and are just as indispensable there as in the cardiovascular system. Hence, pathologies on their part can cause serious disorders disturbing human homeostasis (4). Experimental studies have disclosed that mutations of single nucleotides give rise to pathological conditions, spanning from Parkinson's disease to hyperekplexia (5). Mutations of this kind are linked to proteins which misfolded during the folding process and caused a failed plasma membrane expression of transporter, resulting in diminished reuptake (6). Due to their clinical relevance, SLC6 mutants are of interest as pharmacological drug targets. One possible way to rescue the folding-deficient transporters is by employing chemical and pharmacological chaperones (7). These approach has been met with successful stories the past decades, as mutants in the SLC family were saved following a chaperone treatment, marking them as promising in novel drug development (8).

1.1 The SLC6 protein superfamily

The SLC6 transporters comprise a group of NSS which operate by a sodium-gradient. Depending to the carried substrate, there are four groups: 1) neurotransmitter transporters (NTTs), 2) osmolyte transporters with betaine (BGT1) and taurine (Taut), 3) creatine transporters (CRT), and 4) orphan transporter (9). As the name suggests, NTT primarily facilitate synaptic signalling, which revolves around particular transmitters. The corresponding transporters encompass two glycine-transporter, three monoamine-transporters (MATs) – for noradrenaline, dopamine (DAT) and serotonin (SERT) -, transporters for γ -amino-butyric acid (GAT), amino acid transporter for proline and amino acids, and cationic and neutral amino acid transporters (10).

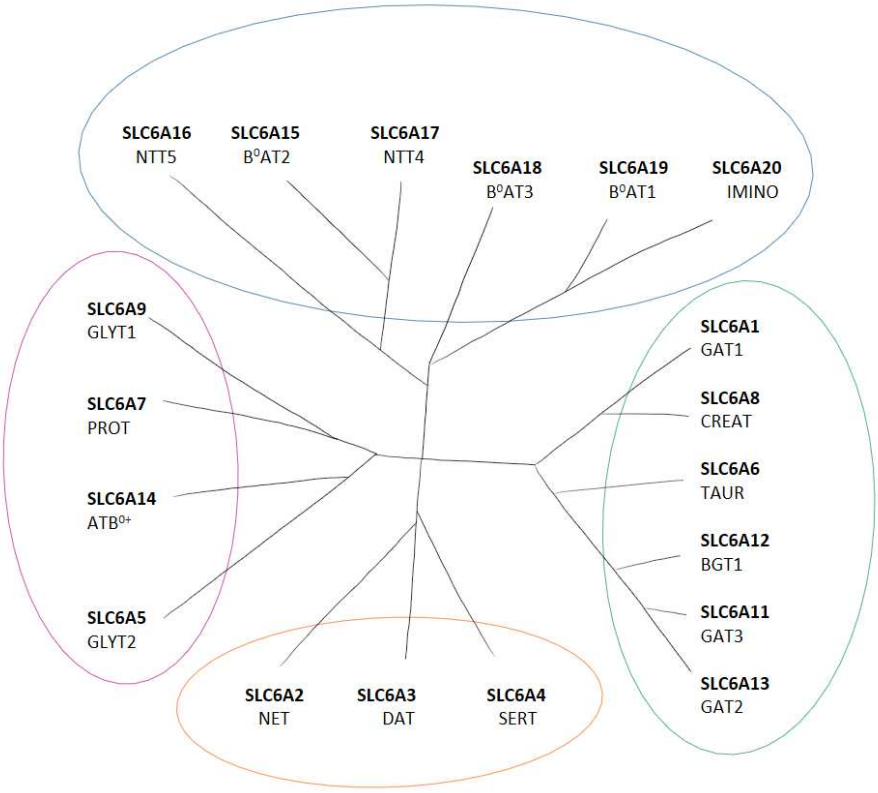

Figure 1. Phylogenetic tree of the SLC6 protein family.

The SLC6 family differs four subgroups with individual members. The orphan group is circled in blue, the amino acid group is seen on the left hand side in violet, the GABA group is on the right hand side in green and the monoamine transporters are encircled in orange. As for the NTTs, they are found in the groups coloured in violet, orange and green.

All these transporters possess 12 transmembrane domains (TMD). The N- and C-termini are directed intracellularly with extended termini, which are likely associated with protein trafficking and ion modulation (9). The termini possess phosphorylation sites as much as glycosylation sites for the purpose of post-translational modifications. On the extracellular side an elongated loop 2 domain (EL2) and another extended loop between TMD3 and TMD4 bearing a disulfide-bridge are present (4). The TMDs are organized in two pseudosymmetric segments, first one formed by TMD1 to TMD5 and the second by TMD6 to TMD10. TMD11 and TMD12 lay outside these segments. TMD1, TMD6 and TM12 are broken into two helices each of 1a and 1b, 6a and 6b, as well as 12a and 12b (11). All these TMDs are cellularly constituted in a way that allow the binding of Na^+ and substrate towards their respective binding sites: Na1 and Na2 for Na^+, and S1 for the substrate (11). A putative S2 has been postulated for MhsT as an allosteric substrate site (S2) and has acquired various functionalities the past years (3, 8). In the end, it is still unclear what exact significance lies in S2, whether it is merely an allosteric binding site for substrates as well as for inhibitors, or an indispensable moiety for reuptake (9).

The bindings sites are located within the first 9 TMDs and facilitate a concurrent transport of both ion and substrate once occupied (12). In terms of reproduction of the quaternary assembly of TMDs, difficulties arose as the transporters immediately change their confirmation once apart from the natural milieu (13). Yet, molecular modelling was a necessary step to gain knowledge in the mechanism of transport as well as substrate-structure-relationship (9). The prokaryotic leucine transporter LeuT, found in the bacterium *Aquifex aeolicus*, is the first identified homolog of the eukaryotic SLC6 transporter (14). It has provided sufficient insight on the NSS crystal structure and firstly allowed to determine the multiple confirmations substantial for substrate transport (4). Further research has provided more structural homologs like the prokaryotic multihydrophobic substrate transporter MhsT from *Bacillus halodurans*, DAT in *Drosophila melanogaster* and SERT, that confirmed and refined the transporter data obtained from LeuT (15).

All four models conserve four oligomeric stages during substrate transport: outward-open, outward-occluded, inward-occluded and inward-open. MhsT, as the most recent SLC6 homolog, has a scaffold formed by TMDs 3, 4, 5, 8, 9 and 10, similarly to LeuT, which are embedded in the lipid layer (4). The remaining TMDs 1, 2, 6 and 7 form the mobile bundle as they enable the switch from outward-occluded to inward-open state for release (12). Especially the two-helices TMDs 1 and 6 are indispensable due to their significant contribution to gate

formation and substrate trafficking (16). The external gate, which is formed by the TMDs 1b, 3, 6a, 8 and 10, contains the primary substrate pocket and allows polar interactions between the substrate and chemical groups of similar properties in TMD1b and TMD6a (12, 17). Hydrophobic moieties undergo hydrophobic interactions with molecules located in TMDs 3, 8 and 10, which assist in gate closure (17). This step keeps any more compounds from entering.

The simultaneous binding of Na^+ triggers a conformational change of TMDs 1b, 6a, 7 and the EL4, that lies in close proximity to TMD1b (12). EL4 together with TMD1a, the intracellular TMD1 segment, prime the substrate release by directly communicating with TMD5, the N-terminus and the Na^+ located in Na2. The ion keeps TMD1a firm and sets loose once confirmation changes in the extracellular compartment occur. TMD5, which is tightly held by TMD6a, unwinds as soon as TMD6a shifts and enforces an inward-open state (12). This grants water molecules access to Na2 and induces release of the ion into the cytoplasm. TMD1a is unbound and allows cumulative release of substrate and the other Na^+ (14, 16). When it comes to TMD6b, its contribution to intracellular opening does not seem to be as relevant as compared to TMD1a (18).

Interestingly, eukaryotic NSS depend on a Cl^-, whereas the prokaryotic models MhsT LeuT operate without such (19). The binding site is comprised of TMDs 2, 6a and 7 and includes polar groups which interact with the ion. While MhsT solely relies on the sodium gradient, LeuT exhibits glutamate (E290) as the acidic equivalent (18). However, the Cl^- dependency had been investigated in a LeuT model, where a negatively charged molecule was substituted with serine, a protein present in MATs at the respective site. This experiment in turn had shown the subsequent decrease of transport and hence proven the transport process to be also coordinated by Cl^- (20). Studies have also stated the Cl^- dependence of antidepressants in particular: The mutation of serine in a NET model lowered the affinity of desipramine due to deficient Cl^-binding, while other models of SERT had shown improved binding of antidepressants (20). Yet on the other hand, another experiment had shown that as soon as SERT was Cl^- independent, antidepressants were also devoid of Cl^- dependency and acted without its presence (18).

This illustrates the complexity of the transporter well, especially if we consider the present differences between the prokaryotic and eukaryotic models. However, the prokaryotic transporters are crucial for our understanding and set indispensable examples for research of NSS (13).

1.2 The Norepinephrine Transporter

NE, also known as noradrenaline (NA), is an endogenous molecule that operates both as neurotransmitter and hormone in the body. As part of the catecholamine group, NE is active in physiological responses to dangers and emergencies. When it comes to central functioning, NE increases arousal, alertness, and attention. In order to regulate these activities in the synaptic cleft, its presynaptic transporter NET terminates signalling by constituting neuronal reuptake. This regulation is crucial to assure proper neurotransmission and prevents unrestrained stimulation of postsynaptic neurons (21). In this context we may also recognize its pathological properties, spanning from psychiatric diseases like schizophrenia and attention deficit hyperactivity disorder (ADHD) to cardiovascular diseases such as orthostatic dysregulation or hampered baroreceptor reflex. NET has been target for different diseases and, therefore, exploited for pharmacological treatments (22).

The transporter is predicted to constitute 617 amino acids in a 12-TMD-assembly, containing intracellular N- and C-termini just like the other SLC6 members. It is solely found in noradrenergic cells including glial cells, adrenal medulla and lungs (23). In terms of stoichiometric properties, NET acts as a symporter for two Na^+ ions, one Cl^- ion and NE. Using hSERT and dDAT, a crystal structure for hNET was converged and allowed to conduct comprehensive studies on binding sites relevant for a transport (24).

The extracellular gate is supported by TMDs 1b, 3, 6a, 10 and EL4, with certain residues (Arg80, Arg81 in TMD1b, Gln314 in TMD6a) significantly contributing to substrate uptake (25). Concerning the primary binding pocket, the substrate binding occurs between TMD1, TMD3, TMD6 and TMD8, with hydrogen bonds and hydrophobic interactions securing the substrate in S1 (24). These bonds are mediated in three different subsites: A, B and C. While A (lined by TMDs 1b, 6 and 8) corresponds to the binding site for the amino group, B captures the hydrophobic portion of the molecule with TMD3 and TMD8 (11). As for subsite C, located between the two segments of TMD6 and TMD3, it seems to extend a vicinity for drugs, especially inhibitors (26). The type of ligand binding the TMD6 linker responds with a respective repositioning of the TMD, resulting either in uptake or inhibition (26).

Once a molecule enters the binding pocket, TMDs 1b and 6a tilt towards TMD10 and initiate a closure of the extracellular gate (11). TMD10 triggers a shift of TMD9, which eventually loosens the interactions between the TMDs forming the intracellular gate and concludes with

an inward-facing opening (24). The simultaneous binding of Na^+ in Na1 is substantial for transport as the cation coordinates the substrate in the binding pocket (21). Comparably, an occupied Na2 site eases the transition from an outward-occluding to an inward-facing constitution and aids in substrate release as water molecules dissolve the cation from Na2 into the cytoplasm (25). This allows a rearrangement of EL2 along with EL4 and alters the position of the N-terminus, followed by a destabilization TMD5. TMD1 unwinds subsequently, providing an opening for the substrate to be eventually released into the intracellular compartment (27).

A potential S2 resides among the ELs 4, 6 and the TMDs 1b, 6a as well as 11, which might also act independently from the primary binding. Essential appears to be the flexibility generated by TMD6, which enables the adaption of domains to structure (26). In this regard data are not yet definitive, however, the knowledge of a possible allosteric site sets a target for drug development to grow, demonstrating how important the understanding of NET is, on top of that in drug development (9).

1.2.1 Synthesis of NE

The name (L-) Norepinephrine derives from the Greek language while the roots for (L-) Noradrenaline lay in Latin. The meaning for both names is the same though, as they lay in the location of synthesis: the suprarenal gland, to be exact the adrenal medulla. Norepinephrine (NE), as the name implies, is closely related to the hormone epinephrine or better known as adrenaline. The key distinction lies in the absence of the N-methyl group in NE. Although so small, the missing carbon-group makes a huge difference in receptor-affinity, on the hand because of the additional arm, on the other handy due to the missing, respectively the missing, hydrophobic moiety provided by the methyl group (28).

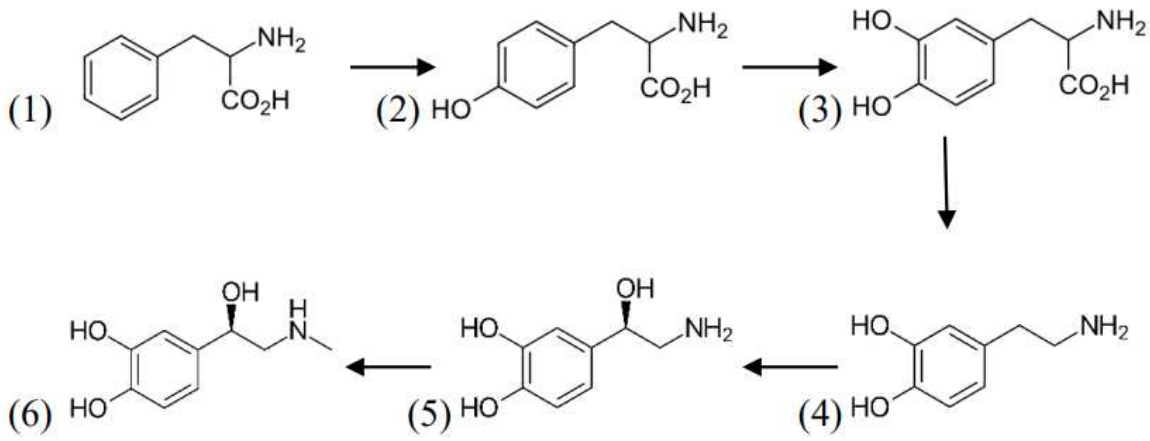

Figure 2. Synthesis of NE and epinephrine.

The first step sets the amino acid phenylalanine (1) as it is hydroxylated to tyrosine (2). The enzyme tyrosine hydroxylase adds another hydroxy group to tyrosine in order to generate L-DOPA (3) which is followingly decarboxylated to dopamine (DA) (4) *via* a DOPA decarboxylase. The steps after concluding the synthesis of NE (5) with a β-hydroxylase, and for adrenaline with an N-methyltransferase.

As for the way up to NE, the synthesis starts with the aromatic amino acid (L-) Tyrosine. Tyrosine hydroxylase is a key enzyme in the synthesis of catecholamines, a group of aromatic compounds whose name is derived from a aminoethyl-chain attached to a catechol (a benzene with two hydroxyl groups) (22). The enzyme hydroxylates (L-)Tyrosine to (L-) Dihydroxyphenylalanine (L-DOPA), which is further broken down into DA with the DOPA decarboxylase. NE is eventually acquired *via* dopamine β-hydroxylase and is subsequently kept in the synaptic vesicles.

1.2.2 Physiological role

After exocytosis, NE binds on its respective receptors and initiates further signal pathways depending on the type of triggered receptor. In order to prevent any excessive signal transmission, the synaptic cleft must be emptied from the catecholamine. For this sake neurons possess NET, which direct the most common route of NE removal (29). The transporters are located in the presynaptic plasma membrane and serve the purpose of concentration regulation

in the synaptic cleft. Once NE is taken back into the presynaptic neuron, it follows either degradation or will be stored in vesicles *via* vesicular monoamine transporter 2 ($VMAT_2$). This process can be summarized as a cycle of NE release through exocytosis and NET-mediated reuptake (25, 26).

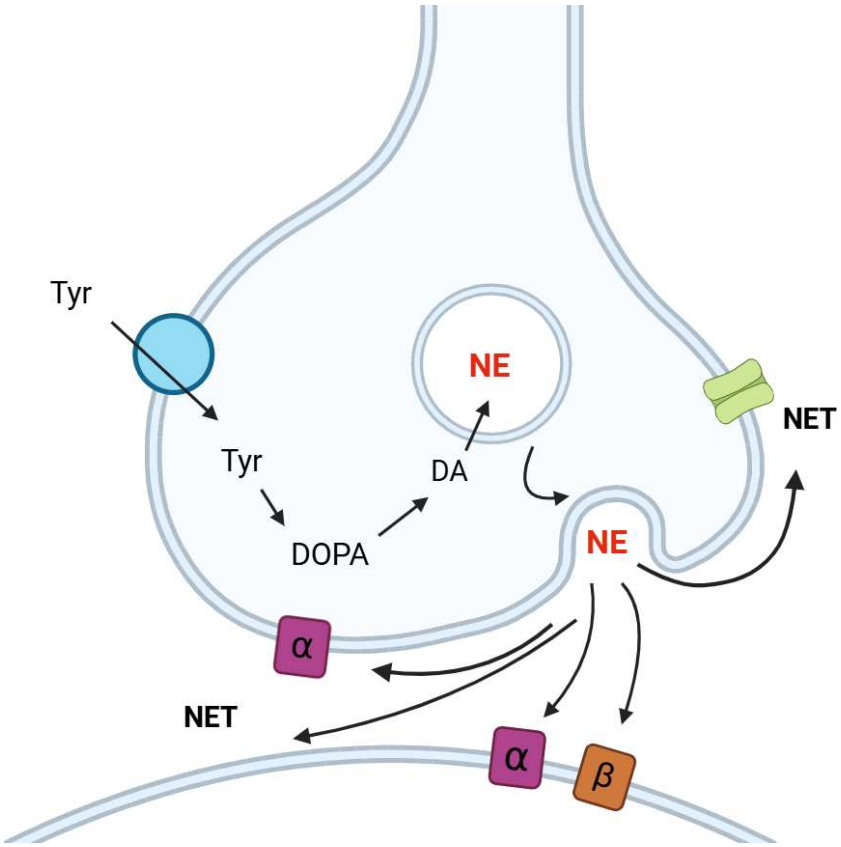

Figure 3. Diagram of NE synthesis and exocytosis.

Tyrosine (Tyr) is first transported into the nerve cell for synthesis of NE. The amino acid undergoes various enzymatic reactions on the way to the neurotransmitter, including a state of DOPA, which is then converted to DA. DA is transported into the vesicle, where it is converted to NE. Once the release is initiated, NE binds to several receptors: α_1, α_2, β_1 and β_2 (the members of both receptors are summarized here in α and β). α_2-receptors are present on the presynaptic membrane for autoinhibition of NE release, while the other receptors are expressed in the postsynaptic membrane. Reuptake is induced by NET, present in the presynaptic membrane as well as on the extraneuronal membrane.

NE depletion by NET is of enormous importance as around 80% of its removal is covered by the transporter (23). It substantially controls arousal, mood, focus and memory, but not only

that, its role in the endocrine as well cardiovascular activities makes it even somewhat vital to have the neurotransmitter regulated. This supports the notion that an impairment of NET and disruption of NE uptake can lead to significant physiological and psychological disturbances (19, 25). The associated diseases will be explored in a later chapter of this thesis.

1.2.3 Ligands of NET – exogenous vs endogenous, agonist vs antagonist

NE is considered an endogenous ligand, as its naturally produced in living organisms. In contrast, exogenous compounds are introduced from external sources but still bind to the same receptor. When considering those from outside, we distinguish two categories: NET agonists and NET antagonists. Agonists induce NE uptake, reducing NE levels in the synaptic cleft. Conversely antagonists elevate the NE concentration by NET inhibition. Agonists mainly include fluorescently labelled NE-derivates, which are used to mark the transporter and utilize for further research purposes (31). Yet, amphetamine is one of the few NET agonists that is available as a prescription drug. The pharmaceutical is used for ADHD and narcolepsy, as it regulates the release and uptake of monoamines in the CNS, treating the underlying problem of both diseases (32). However, the increase of NE availability also leads to physiological stress response as well as euphoria. Due to these effects, amphetamine is heavily abused as a pleasure drug with severe health consequences leading up to life-threatening conditions and death. Cocaine is another highly addictive compound of the tropane group that, in contrast to amphetamine, exerts inhibitory effects. The inhibition of MAT provides similar effects to amphetamine misuse, which is why it is applied only under certain circumstances (33).

Speaking of NET inhibitors, they are pharmacologically and clinically very appealing as they have proven to be exceptionally effective in a wide range of diseases. For instance, atomoxetine as an NET inhibitor effectively manages the case of ADHD (34). Success in the development of antidepressants has shown, that patients suffering can be minimized if the right treatment is performed. This chapter serves to characterize Amphetamine, Cocaine and antidepressants in their functionality, focusing on substrate-receptor-activity, endogenous effects and pharmacological significance.

1.2.4 Amphetamine

When looking at their chemical structural, the similarity of catecholamines and amphetamine (and derivates) immediately strikes the eye. As part of the Phenylethylamines, the psychostimulant harbours a phenylic ring with a nitrogen atom connected to it *via* the ethyl chain, which makes it a competitive substrate for MAT (35). The drug is transported through the Na^+ gradient from extracellular to the intracellular space, where it is consequently stored in vesicles. Once inside the presynaptic cell, it prevents the vesicle packing of neurotransmitter by competitively binding $VMAT_2$. The failed translocation of neurotransmitter indicates an increase of cellular monoamine concentration, that eventually causes its release into the synaptic cleft, a process referred to as "reverse transport" (35). The mentioned effects are complemented by reuptake inhibition, though weak, and degradation inhibition through the monoamine oxidase (MAO), an enzyme that catabolizes DA, NA and Adrenaline to their deaminated products (36). This activity is relatively weak hence it might occur when amphetamine is intracellularly concentrated (35).

As mentioned above, amphetamine is legally prescribed to treat ADHD and narcolepsy, it can even be used as an appetite suppressant in treatment of obesity. The synergistic activity of all mechanisms increases the monoaminergic neurotransmission and maybe even serotonergic signalling that often ails the conditions of ADHD with anxiety or depression (35).

1.2.5 Cocaine

The tropane-based alkaloid is naturally contained in the leaves of the coca plant *Erythroxylum coca*, native to South America. In 1880, it was initially demonstrated by Carl Koller (1852-1925) as a surgical anaesthesia and soon after gained positive responses from all over the world (37). Aware of its euphoric qualities, the coca plant was ingested by the indigenous population to combat fatigue and cut energy expenditure – marking the beginning of addiction and abuse (38). Depending on the dosage and route of administration, the drug elicits either immediate or retarded effects. Pharmacologically it features high affinity for NET, SERT and especially DAT, whilst blocking reuptake of the respective neurotransmitter (39). The accumulation in the synaptic cleft amplifies the neurotransmission, ending in long-term adaptation if consumed regularly. In case of short-term-effects the tropane alkaloid exhibits behavioural changes

(mainly mediated by DA), arousal and alertness (as a result of NA increase), irritability, heightened blood pressure and if consumed in higher doses, irritability, anxiety, aggressivity and paranoia (38). Long-term indulgence of cocaine, as studies report, might substantially trigger neuroplasticity of glutamate releasing nerves. On the route to figuring out the meaning if this change, it has been registered that addiction is highly dependent on exactly glutamate release, which additionally activates dopaminergic receptors (40). The glutamate system might become a target to inactivate cocaine-induced addiction concomitantly to treatment.

Apart from its therapeutical significance, cocaine may cause severe cardiovascular complications all the way to cardiac arrest and sudden death. Hence, the drug is strictly prescribed and consumed solely under medical supervision (38).

1.2.6 Antidepressants

This group of drugs is prescribed for patients suffering from not only depression, but also obsessive-compulsive-disorder, social phobia, schizophrenia, panic disorder, posttraumatic stress disorder and many more (34). Based on their mechanism of action, we distinguish different types of antidepressants: serotonin-norepinephrine-reuptake-inhibitor (SNRI), selective serotonin reuptake inhibitor (SSRI), atypical antidepressants, norepinephrine and specific serotonergic antidepressants (NASSA), tricyclic antidepressants (TCA), monoamine oxidase inhibitors (MAOI) and atypical antidepressants (41). The notion of pharmacological targeting of transporters rose from the so called monoamine hypothesis, which implies that a deficit of NE and serotonin, chemically known as 5-hydroxytryptamine (5HT), reduces postsynaptic signals and promotes pathological diseases. However, current data suggest otherwise: In case of tianeptine, for example, the induction of 5HT reuptake rather works against anxiety and depressive disorders, and for healthy probands another study had shown that a deficit of monoamines did not affect their behaviour and mood (42). This information gathered over the past decades make the theory less legitimate, hence more research in the field of psychological and psychiatric disorders is required.

Followed by the monoamine hypothesis, the first antidepressants evolved: MAOI shall inhibit the cleavage of monoamine to promote their increase in concentration, and TCA inhibit SERT and NET. More commonly used drugs are currently the descendants of TCA, SSRI and SNRI. Examples for SSRI are paroxetine, sertraline, escitalopram and fluoxetine, meanwhile SNRI

include venlafaxine and duloxetine (34). Unlike them, atypical antidepressants involve various mechanisms of action, affecting not only NE and 5HT reuptake but also including inhibition of DA reuptake like bupropion does or blocking α_2-receptors mediated excitatory signals *via* mirtazapine. Agomelatine works as an agonist for melatonin-receptors, but synergistically promotes NE and DA release by blocking the 5HT2C-receptor (43).

First line therapy for depressive disorders is SSRI due to their high effectiveness. SNRI act just as effectively on both SERT and NET, simultaneously attacking two groups of interest in the field of psychological disorders. First visible relieve, though, can take approximately 2-4 weeks and still does not assure prosperous effects for all individuals. Especially the range of adverse effects following intake of SSRI and SNRI heavily impacts an individual's life. Therefore, knowledge of novel data undermining the monoamine hypothesis makes it obvious that latter is merely a simplistic view of the complex nature of mood disorders. Therefore, novel approaches have become a necessity to target the disease (44).

1.3 The GABA Transporter

GABA transporters play a fundamental role in CNS functioning by supporting the system to maintain a healthy level of synaptic GABA concentration. Along with Na^+ and Cl^-, GABA works as an inhibitor *via* $GABA_A$ - and $GABA_B$-receptor to diminish further neuronal excitability and thus, facilitate the balance of excitatory and inhibitory neurotransmission (45). However, overstimulation of GABA-receptors needs to be terminated in order to prevent continuous inhibition and allowing regulation of neuronal circuits again (46).

Depending on their location, those neuronal circuits can be managed by 4 different types of GABA-transporter each expressed by individual genes: GAT1 (SLC6A1), GAT3 (SLC6A11), BGT1 (SLC6A12) and GAT2 (SLC6A13) (9). GAT1 is most dominant in central presynaptic neurons, particularly high expression can be found in the neocortex, hippocampus, cerebellum, basal ganglia, brainstem, spinal cord, olfactory bulb and retina (4). Compared to the first transporter, GAT3 displays rather high activity rate in glia cells, whereas GAT2 is much more distributed in arachnoid and ependymal cells, showing hardly any presence in neurons and glia cells. BGT1 is expressed in lower levels in the CNS but predominantly found in the liver (45).

Table 1. Members of SLC6 with corresponding transporter, substrate and known pathologies

Human gene	Transporter	Substrate	Pathological conditions
SLC6A1	GAT1	GABA	Epilepsy, schizophrenia, ADHD, autism(47)
SLC6A11	GAT3	GABA	Epilepsy
SLC6A12	BGT1	GABA, Betaine	Epilepsy
SLC6A13	GAT2	GABA	Epilepsy

GAT1 has been greatly studied compared to the other SLC6 transporters due to its involvement in severe neurological and psychiatric diseases, e.g. epilepsy, autism, Alzheimer's disease, stroke and schizophrenia (48). Even associations between BGT1 and neuropsychiatric patterns have been made, such that interest has surfaced for BGT1 as a potential drug target, especially in epilepsy. Yet, lacking evidence and its controversial expression in CNS rise questions regarding its relevance (45). GAT1, as the major isoform of its group, is accountable for 75% of total GABA uptake, whereas the other ones fill up the remaining percentage (49).

As a member of SLC6 carrier, GAT1 adopts the conformations outward-open, occluded-out and inward-open. The outward-open confirmation has Na^+ ions bind to their respective sites, attracting GABAs as well as Cl^- ions consequently. Latter maintains the intracellular neutrality. This step is followed by the occluded state, which restricts excess binding of substrate. The next conformational change constitutes an inward-open state through angling of TMD1a, allowing GABA and ions to drift off GAT1 into the intracellular compartment (49).

A rat GAT1 was engineered to generate a human GAT1 (hGAT1) and utilized for cryo-electron microscopy, a technique often used for assessing quaternary structures like receptors *et cetera* (50). This model has confirmed TMDs 1, 6, 3 and 10 to greatly influence uptake of substrate. The extracellular gate closure is mediated by Ser456 in TMD10, which at first widens the uptake space. Its hydroxyl group interacts with the hydroxyl group of Thr29 in TMD6, closing the pore. The increased presence of hydrogen bridge bond is required in order to retain substrate-pocket-interaction (49). Na^+ in this matter is substantial as it stabilizes the outward-open state for the substrate and Cl^- ions to bind (51). As soon as they join, the transporter enters the occluded state, presumably achieved by the phenylic acid Phe294 and Tyr140, that sever

any connection to the extracellular space (50). Cl^- ions seemingly assist in gate closure through TMDs 1 and 10 (52). Concerning the binding pocket, the so called subsites A, B and C initiate substrate recognition. There GABA is accordingly set to facilitate the pore opening towards the cytoplasm. An indispensable residue seems to be Ala455 in TMD10 which forms a π-bond with the amino acids Ser456 or Gly457, located in the same TMD, and again interact with TMD6 residues to allow a intracellularly open gate (50). This step is assisted by an unwinding of TMD5 as well as TMD7 while TMD1a navigates to an open state. This way the substrate is ultimately released (53). Right after, Cl^- dissociates and the emptied transporter is ready to instigate a new cycle (54).

1.3.1 Synthesis of GABA

GABA is produced in GABAergic neurons across various brain regions. The initial step is set by glucose which is converted to α-ketoglutarate after several steps of Krebs-cycle. α-Ketoglutarate is then converted into (L-) glutamic acid through transamination that is catalysed by the enzyme α-oxoglutarate transaminase. The final step is completed with a decarboxylation of (L-) glutamic acid induced by the equally called enzyme glutamate decarboxylase (55).

GABA is kept in vesicles for a for the vesicular release. Once in the synaptic cleft, GABA can be degraded either in the presynaptic neuron or in the neighbouring glia cells. The enzyme GABA transaminase then forms succinate semialdehyde, which eventually enters the citric acid cycle (56).

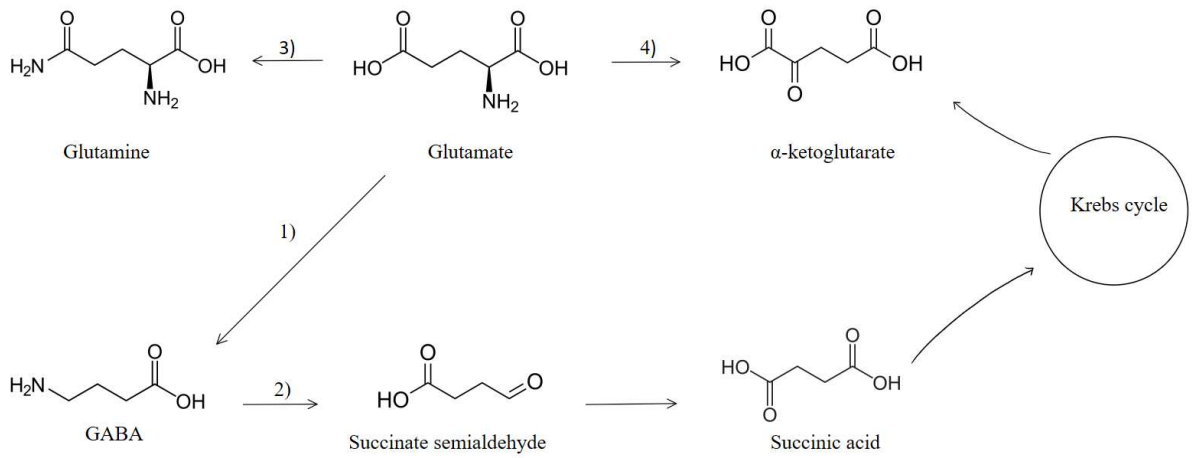

Figure 4. GABA synthesis and degradation.

The glutamate decarboxylase (1) degrades glutamate to the transmitter in question, GABA. GABA Transaminase (2) transforms the GABA to succinate semialdehyde, which is then degraded to succinic acid. The latter is henceforth involved in the Krebs cycle. For glutamate, glutamine synthase (3) generates the amino acid glutamine, whereas glutamate dehydrogenase (4) generates α-Ketoglutarate. This substrate can also be gained from the Krebs cycle.

1.3.2 Physiological roles of GABA

GABA is the primary inhibitory neurotransmitter in mammals, being of foremost importance as it regulates the neuronal excitability initiated by neurotransmitters, particularly by glutamate. Its presynaptic transporter GAT serves as the main mechanism for clearing the synaptic cleft from high GABA concentration, managing around 75% of the extracellular GABA levels (48).

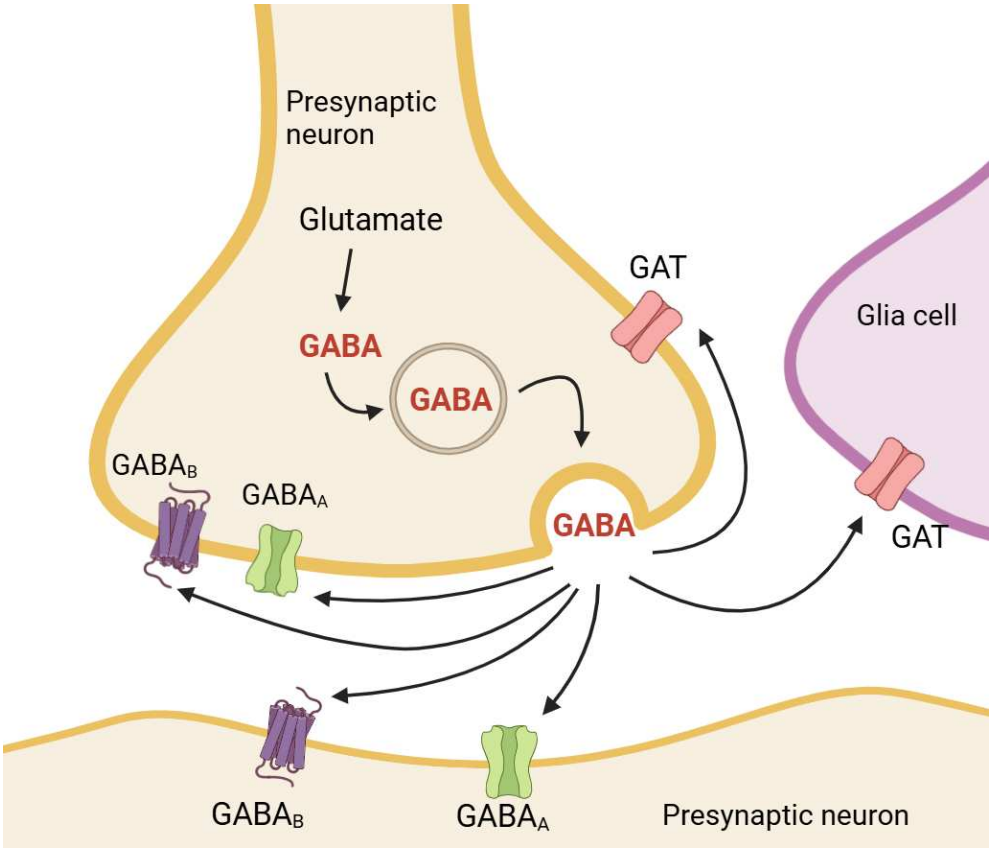

Figure 5. Illustration of GABA synthesis and exocytosis.

Glutamate is converted to the neurotransmitter GABA, which subsequently enters the vesicle. The vesicle interacts with the presynaptic membrane to initiate the GABA release and induce signalling. $GABA_A$ or $GABA_B$ induce inhibitory signals on the subsequent neurons once the neurotransmitter binds, whereas GAT modulates the signalling by transporting it back to the presynaptic neuron. GABA can also be transported into the glia cell *via* GAT but enters the metabolism pathway.

As already mentioned above, GAT1 is more abundant in neuronal regions than in glia cells. Particularly hippocampus, cerebral cortex, cerebellum and basal ganglia express a higher concentration (48, 57). Following exocytosis, GABA acts on its respective receptors, GABA-A and GABA-B, and transmits inhibitory signals to modulate postsynaptic excitability. Right after, the neurotransmitter is taken up by GAT1 in order to prevent excessive tonic activation and kept in the presynaptic vesicles (57). A small portion of GABA lands in surrounding glial cells where, unlike presynaptic cells, no GABA is reutilized for release but degraded (49).

1.3.3 Ligands of GAT1

The high expression of GAT1 marks it as an important pharmacological target in the innovation of new drugs. Considering that, we differ agonists, triggering GABA uptake, and the more common antagonists, blocking its uptake. Per definition, agonists enhance the intrinsic function of GAT1 to replenish neuronal GABA concentration. Their use as pharmaceutical drugs is yet little to none and rather serve as experimental and analysis instruments (58). GAT1 inhibitor, or GAT inhibitors in general are of greater interest in the field of drug development. As they increase extraneuronal GABA availability, these inhibitors have been deemed as highly effective in the treatment of epilepsy, joining the group of anticonvulsants (49). This chapter discusses the importance of agonist as well as antagonists and how their properties were and will be utilized for the sake of research and novel therapy.

1.3.4 GAT1 substrates

Similar to NET, GAT1 agonists serve as a way to improve understanding of GAT1 and its ways of functioning. Several years have been invested to develop radioligands that might aid in GAT1 imaging – however, without success. Few have been propagated but certain chemical traits devoid the compounds of brain permeability. It was found that the amino and carboxylic groups seem problematic due to their zwitterionic nature, however, are indispensable for receptor-ligand-interaction. Cyclic GAT1 antagonists like nipecotic acid and guvacine were promising candidates as they are structurally like GABA which is why they were accordingly facilitated for ligand synthesis. The additions of a *N*-alkyl-chain and carboxylic ester were expected to remove the zwitterionic behaviour and benefit blood-brain-barrier (BBB) passage – again without success as no uptake was registered in rat brains (54, 55). In the case of GAT1 inhibitors, prolonged lipophilic chains provided increasing affinity for the hydrophobic region in substrate binding site. This will not be successful for radioligands as we desire a reuptake of our ligand instead of inhibition. For this reason, the idea of bioisosteres was proposed followed by surprising results: an increase in brain permeability and uptake was registered. Bioisosteres of carboxylic acid seem to present a new strategy for radioligands and therefore need to be analysed more extensively (58).

1.3.5 GAT1 inhibitors

In terms of GAT1 antagonism, we have previously discussed two GAT1 antagonists applied in radioligand synthesis, nipecotic acid and guvacine. Both comprise a nicotinic acid scaffold compared to the endogenous ligand, which strengthens their inhibitory potency. Particularly nipecotic acid displays strong inhibition as *in vitro* studies report. Due to its polar nature, though, overcoming hurdles like BBB penetration or ion-ion-interactions rendered its use as pharmaceutical drug impossible (60). Therefore, modification and optimization experiments were conducted and eventually enabled marketing of the sole GAT1 blocker: tiagabine. The hydrogen atom on the piperidine-*N* was replaced by a lipophilic chain which in turn resolved the problem of blood-brain-permeability (60).

Table 2. chemical structures of GAT1 antagonists

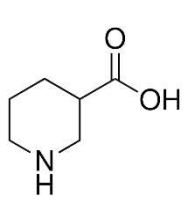

Nipecotic acid

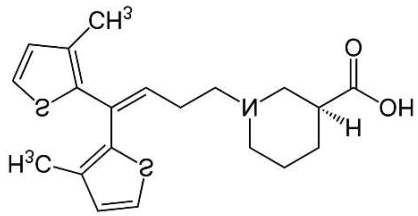

Tiagabine

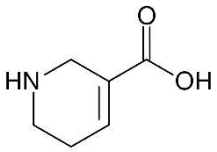

Guvacine

Nipecotic acid competitively blocks the GABA binding site by preventing a conformational change of TMD1a and TMD5, which normally unwind after substrate contact. Tiagabine equally blocks the transporter, with the slight difference that TMD1a and TMD5 bend away from their innate location. The unwinding is related to the lengthy side chains of tiagabine and the thiophenylic group (60). The inhibition potential nipecotic acid and success met with tiagabine gave rise to the hope that derivates might give results like tiagabine. However, clinical trials of various compounds ended up with serious adverse effects and eventually had to be discontinued (49). Other antagonists are NNC-711 and Cl-966 which are modified guvacine derivates. These inhibitors performed just as effectively as the nipecotic acid derivates in *in vivo* studies, where mice models were followed by a relief in seizures. However, no more studies were performed afterwards (58).

1.4 Protein quality control mechanism of hNET and hGAT1

Proteins undergo a bunch of post-modifying corrections to ensure their proper functioning. In regards to the group if SLC6, analysis of amino acid sequences confirm that several protein modifiers, such as protein kinase or glycosylation processes, determine the transporter-specificity and subsequent allocation of transporter (61). Especially the Endoplasmic Reticulum (ER) has been thoroughly studied in respect to the solute carrier family, as it is greatly involved in oligomerization of GAT1, MAT and more (62). This cell organelle is involved in two substantial steps: first of all the most primary of all peptide modification, namely folding and maturation, while the second step incorporates the transporter export from the ER (62).

1.4.1 Protein folding – the proximal quality control

Folding, respectively oligomerization, of polypeptides follows no particular pattern, but more or less relies its trajectory pathway on the energetically best conformation. As we know, atoms follow the state of lowest, hence, most stable state (63). In order for the protein chain to reach this low level of energy, it is subjected to many complex folding trajectories, containing rearrangements of hydrophobic parts in the polypeptide to adjust to the lipophilic milieu within the ER membrane and adaption to the SEC61 translocon channel, which is responsible for the transport in the first place (64). These complex processes put a major strain on the native chain in terms of high energy states, thus, the protein requires native chaperones to help the 12 domain chain take on a correctly folded transporter (65). In contrast, abnormally folded protein follow the way of Endoplasmic-Reticulum-associated-degradation (ERAD) (2).

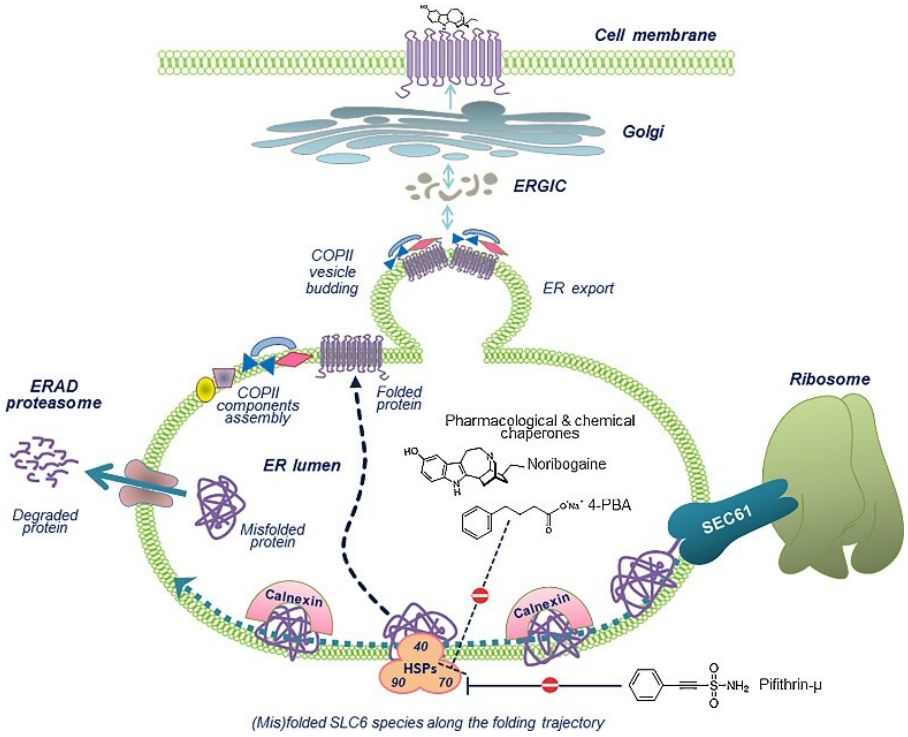

Figure 6. An illustration of transporter export from the ER.

The post translational protein chain is transported to the ER through SEC61 translocon. It interacts with the hydrophobic segments of the polypeptide chain in order to allow a smooth entry to the ER lumen. The glycosylated transporter moves towards the calnexin/calreticulin complex before relaying to the HSPs. At this point, the transporter is either conveyed to coat protein complex II (COPII) for export, or in case of a misfolded structure transmitted for degradation. When feasible for export, the transporter enters the Golgi apparatus through a vesicle budding mechanism that is mediated by an assembly of COPII components. It first enters ERGIC before reaching the Golgi apparatus. The depicted chaperones pifithrin-μ (2-phenylethynesulfonamide), noribogaine and 4-phenylbutyric acid (4-PBA) ease the stringent protein quality control and allow transporters for export (2).

When entering the lumen, the lipophilic segment goes ahead after having passed through the hydrophobic milieu in the ER membrane. However, lipophilic structures tend to aggregate easily. In order to keep them from doing so, luminal chaperones like calnexin and calreticulin stabilize the native conformation (66). Both possess glycan-binding lectins that specifically assist in folding of glycosylated N-termini (67). Upon protein glycosylation, the N-domain has two of its monosaccharides removed by glucosidase I and II, which generate an N-monoglycosylated terminus. In this state the protein eventually binds the lectin site and calnexin/calreticulin can ultimately commence the folding (2, 68). If the correct conformation

is not achieved, the enzyme UDP-glucose-glycoprotein-glucosyltransferase (UGGT) re-glycosylates and sends the misfolded protein back to calnexin/calreticulin. Afterwards two possible paths await: Either a correctly oligomerized protein trafficking towards the next stop or the path down to ERAD (67).

1.4.2 Transporter export – The secondary quality control

Once the protein is ready, it will be transported to the Golgi apparatus through an ER-specific shuttle system provided by the COPII. This group comprises a set of membrane proteins called SEC23/SEC24, SEC13/SEC31 and Sar1 which facilitate the budding process from the ER and essentially shape the liposomes (67). Sar1 first binds to ER-resident membrane proteins, with GTP-hydrolysis as ATP-generating step, and allows the SEC23/SEC24 unit to bind subsequently. Followed by SEC13/SEC31, the proteins polymerize and complete the budding with vesicle formation. Last but not least the shuttle follows an anterograde transport to the Golgi system for further modifications (69). The ER-Golgi-pathway in particular has an intermediate relay for protein transport defined as the ER-Golgi-intermediate-compartment (ERGIC). It is a microtubular system for luminal secretory vesicles to exit the ER and connect with the *trans*-Golgi-membrane (67). Upon vesicle-membrane-fusion and post translational sorting the finalized transporters are released from the *cis*-Golgi-system and located to the cell membrane (2).

As of now, COPII vesicles are the most prominent protein carrier to our knowledge as they ensure a high selectivity in ER export: Properly folded proteins move forward while misfolded ones remain in the cell organelle. If in any case cellular dysregulations interfere with proper protein trafficking and eventually disturb cellular homeostasis, further quality control mechanisms will be activated. Especially the interaction of COPII with COPI is speculated to be of great relevance. While COPII vesicles serve the purpose of anterograde trafficking, COPI do exactly the opposite: they translocate the carriage back to the ER and bind to certain receptors or glycoproteins which retrieve the proteins (59, 67). More research is yet to be done in order to give more insights into the kind of receptors or glycoproteins involved and how exactly quality control is mediated, but current knowledge makes the importance of understanding evident – especially if they inhabit potential therapeutic targets.

1.5 Heat Shock Proteins – HSP70 and HSP90

1.5.1 Structure of HSP90 and binding properties thereof

As the name suggests, HSP90 is a proteinous macromolecule which is localized in the cytosol as well as important cell organelles like the ER, mitochondria and the nucleus (71). The macromolecule resides as a homodimer, each arm consisting of an N-terminal-domain (NTD), a middle domain (MD) which then is completed with a C-terminal-domain (CTD) (72). NTD has been proposed as the binding site for ATP, whose hydrolysis is mediated by both NTD and MD, whereas CTD accounts for dimerization (73). The so called charged linker has been described as a link between NTD and MD, solely present in eukaryotic, cytosolic ER and mitochondrial HSP90. Based on its localization the linker is named differently: Grp94 for the first two organelles and TRAP1 connecting the domains for the mitochondrial HSP90. It serves as a binding pocket for regulatory active components, so called co-chaperones, which seem to not only affect the conformational transformation of chaperones, but also coordinate protein stability and the pace of domain arrangement (68, 71). Besides the charged linker between the NTD and MD, another distinctive trait for eukaryotic cells was stated to attract co-chaperones: An extension at the CTD of cytosolic eukaryotic HSP90, harbouring a Methionine-Glutamic acid-Glutamic acid-Valine-Aspartic acid (MEEVD) motif, displays interactions with the super-helical groove of tetratricopeptide repeat (TPR) domains in co-chaperones (71).

Apo-state- HSP90 is mainly conserved in a V-shape, which after ATP-contact, undergoes a number of conformational changes. Because of this flexibility, many forms - like more compact or extended versions - of the protein were declared even in non-apo state (72). Despite the variety. however, one similarity was confirmed by analysing ATP activity on NTD: Once ATP docks on the binding site, the dimerization reaches a stable state by encompassing the tripeptide, catalysing ATP hydrolysis and then the release of ADP + P (72, 73).

However, whether ATP hydrolysis is initiated or regulated, it is mediated by so called co-chaperones. Co-chaperones are non-client-binding proteins, which seem to act as activators and inhibitors for various reactions. An example sets the TRP chaperone Hop, a powerful ATP-hydrolysis inhibitor, which blocks an intermediate state and halts any subsequent reactions. In comparison, Aha1 promotes structural changes (60, 74). Multiple experimental methods like NMR-spectroscopy and crystallization revealed binding points for Aha1 on MD and NTD. This

catalyses a closed conformation of HSP90 and in turn accelerates ATP breakdown (71). There are more sets of cochaperones identified as important regulators of HSP90, just as essential as Aha1 and Hop. However, those will not be described in this thesis. Table 3 shows a selection of HSP90 co-chaperones and their respective role in the cell.

Table 3. Selected molecular chaperones with relevance to HSP70 and HSP90 activity.

Protein	**Human gene**	**Function**
Trp2	DNAJC7	Identify HSP70 and HSP90 *via* their domains, possibly facilitating retrograde trafficking from HSP90 to HSP70
Hop	Stip1	Support system for HSP90 and HSP70 reaction, HSP90 ATPase inductor
Chip	Stub1	Tags Protein for proteolysis
Aha1	AHSA1	catalysator for ATPase; consequently induces the conformational changes of HSP90
p23	PTGES3	Involved in client maturation as HSP90 ATPase inhibitor of HSP90 ATPase, serves as an endogenous chaperon
Cdc37	CDC37	Inhibitor of HSP90 ATPase, endogenous co-chaperone
Fkbp52; Fkbp51; Cyp40	FKBP4; FKBP5; PPID	Involved in client protein maturation

Findings from the last few years suggest that “clients”, as in HSP substrates, display numerous binding sites on chaperones. Interactions with all domains were detected, e.g. a glucocorticoid-receptor-binding domain and p53 interact in between of MD and CTD with domain properties, while Tau, a protein mainly present in Morbus Alzheimer, binds to residues of NTD and MD (69, 75).

1.5.2 Structure of HSP70 and binding properties thereof

HSP70 belongs to the same ATP-dependent-group as HSP90 with the same tasks as latter including quality control and cell viability, although, structurally speaking they are of a slightly different built. While HSP90 possesses 3 domains, HSP70 consists of a nucleotide-binding-domain (NBD), which is linked to a C-terminal substrate-binding-domain (SBD) (72). ATP binds in a cleft formed by four subdomains of NBD, whereas substrate binding occurs at one of two SBD-subdomains namely β-sheet-structure. Unlike the first subdomain, the second structure, an α-helix-chain, keeps the substrate from bindings as its "shields" the β-sheet-chain. However, once Apo-HSP90 shifts to an ATP-bound state, the α-helix-chain moves away from its innate position and reveals the client binding spot. Even when left in an ADP-bound state, the lid of α-helix remains removed and dissociation may go smoothly (79). At the terminal C-domain residues an EEVD motif, which acts as an interaction tool for co-chaperones of Hop/Sti1 and Chip types (80).

With the intention of deepening understanding in aspect of conformation, the prokaryotic equivalent DnaK was used. This in turn allowed the "discovery" of two fellow co-chaperones: J-domain proteins (also known as HSP40) and nucleotide-exchange factor (NEF). Whilst J-domain proteins activate ATPase and draw substrate, NEF works on releasing ADP and binding ATP (72). Together with HSP70, these proteins assist in various cellular quality control mechanisms in order to maintain proper cell functions.

HSP70 is involved in numerous processes, mainly related to quality control: (1) it shields proteins from associating with lipophilic molecules and therefore preventing aggregate formations (2) decreases energy barriers to correctly fold proteins, and (3) dissembles already aggregated protein for these to be refolded to their native form again (80). Especially disaggregation seems to unlock a unique mechanism of action, which received the name "Brownian Power Stroke" by Goloubinoff and colleagues (81). They postulated the higher the thermal mobility of HSP70 compared to an aggregate is, the smoother it dissolves the junk of protein (77, 78). The activity of protein folding is rather complex and is dependent on various regulatory protein, such as co-chaperones, which would go beyond the scope of this thesis and not be detailed here. Hence, we will head straight to the collaborative work between HSP70 and HSP90 to provide a brief look over their relevance and later elucidate their pathological role.

1.5.3 HSP90 and HSP70 – A multifarious collaboration?

It has been known for a long time, that HSP70 is deeply involved with Hsp90, especially with protein folding. Bacterial models demonstrate that DnaK first acts to recognize non-native protein to comprise it and afterwards have HSP90 reactivate and remodel the protein to its aspired state. Both steps require the involvement of DnaK co-chaperone like DnaJ (equivalent to eukaryotic J-protein) and ATP hydrolysis otherwise HSP90 wouldn't cooperate with HSP70 and the energy demands will not be met (69, 79). Similar processes were observed for eukaryotic cells with the small addition of Hop (83). It interlinks both heat shock proteins and enables smooth client handover from HSP70 to HSP90. The presence of J-protein in protein-transfer is just as important because of its effect on Apo-HSP70: As soon as the apo-state is replaced by the ADP-bound one, it allows interaction with HSP90 (84).

Physiologically speaking these proteins seem to play a crucial part in protein functioning. So how das the problem of cell toxicity arises? Despite their cell protective effects, HSP70 and HSP90 have been implicated in numerous pathologies, most prominently cancer, neurodegenerative diseases and viral or protozoa caused infection (85). Protein accumulation is heavily neurotoxic and induces disorders like Morbus Parkinson, and Morbus Alzheimer, which show an increase of synucleins and Tau, marker for these disorders. Expression of HSP70 and inhibition of HSP90 show a reduction of synuclein and therefore decrease in neurotoxic substances (86). Depletion of HSP90 simultaneously results in upregulation of HSP70 as well as J-protein to further attenuate cancerous cell growth (87). The same procedure was efficient for amyotrophic lateral sclerosis (ALS) or Huntington disease, where induction of HSP70 indicated less protein accumulation (88). It is obvious that HSP70 induction prevent augmentation of cell toxicity, however, it does not explain why HSP90 inhibition works equally. Increased HSP90 activity is critical for protein stabilization in cancer cells which in turn promotes their survival and growth (86). In conclusion, HSP90 needs to be blocked using appropriate inhibitors. Those appear to be detrimental for cancer cells in particular leading to cycle arrest, apoptosis and no tumour growth (89). HSP70 has also been assigned to encourage oncogenesis by the same processes as HSP90, thereby the respective inhibitors attained similar effects to HSP90 inhibitors (90). The treatment additionally sensitized cells towards other anticancer treatments like radio – and chemotherapy (90). Both inhibitor classes might define a new class of anticancer therapy, however, the lack of successful trials and critical adverse

effects limit their clinical use. This again gives to understand the complexity of molecular chaperone system and the many challenges which arise handling cell-machineries (79).

1.6 Genetics and Pathophysiology of hNET and hGAT1

1.6.1 Genetics and Polymorphisms of hNET

hNET is found on chromosome 16, with exact localization on q12.2 at the longer arm of the chromosome (91). The transporter gene comprises 13 introns an 14 exons encoding 617 amino acids which translate into the molecular structure (92).

There is a generous number of SNPs known today which differ in their expression rate and frequency. The SNPS are found throughout the transporter, located in the transporter loops as much as in the domains (93). However, the association of their location with respective cardiovascular and psychiatric diseases remain a question in need of an answer.

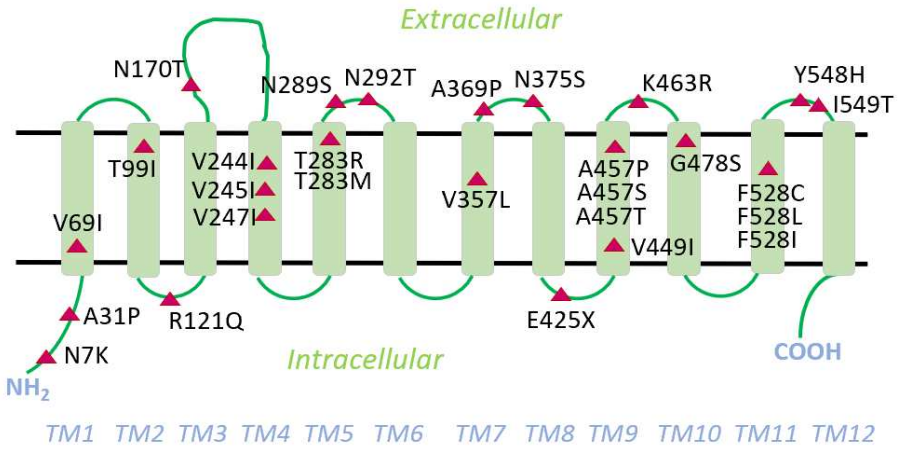

Figure 7. Topology of hNET and known SNPs.

Representation of identified SLC6A2 mutants according to their localization in the TMDs. hNET1 is shown here in a 12-TMD-assembly with both N- and C-termini directed towards the intracellular compartment. The position of mutants is defined in numbers, while the commonly present amino acid is described as a single letter in front of the position number. The letter after the numbers tells the mutant amino acid.

The wild type (WT) hNET possesses five types of alternative splicing, which yield a variety of mutants. One of the resequencing inhabits five missense substitutions with rather low occurrence rate and are the following: V69I, T99I, V245I, V449I and G478S, present in the TMD order 1, 2, 4, 9 and 10. These are known to be expressed in the membrane but possess low affinity for NE (94). A369P and A457P are found in EL4 and TMD9. They are associated with impaired processing to the fully glycosylated form which causes them to be ER-retained. N292T, found in EL3, shows intracellularly kept forms as well as colocalized transporters with a decrease of transport rate by 40%. This equally applies to R121Q, moreover, when co-expressed with WT hNET they even impeded the native transporters functionality. Reuptake reduction to 80% for Y548H accounts for non-significant decrease. Respectively, F528C demonstrated an increased transport activity compared to the WT. This might be due to its insensitivity to down-regulation mediated by Protein kinase C, a common regulator for hNET activity (93). The disease variant T283R lowers its reuptake capacity to 50-70% (6).

1.6.2 Pathophysiology of hNET variants

Numerous pathological conditions were shown to be linked with SNPs in the SLC6A2 group, affecting both the CNS as well as the cardiovascular system. Sufficient data already implicate that most transporters following mutations translate into altered NET activity. Decreased uptake, reduced transmitter clearance and imbalanced synaptic activity altogether increase the chances of suffering from arrythmia, blood pressure dysregulation, ADHD and other conditions interfering with quality of life (91, 93).

In regards to cardiovascular diseases R121Q is the only variant known up to now that causes long QT syndrome, while N292T, V356L, N375S, K463R, F528C, I549T and Y549H are potentially a cause for increased blood pressure (93, 96). A457P is a prominent variant known for its phenotypical presentation in orthostatic intolerance. The case of twin sisters suffering from several symptoms including tachycardia, dyspnoea, fogginess and more revealed abnormally increased plasma level of NE whereas the level of the intraneuronal metabolite dihydroxyphenylglycol (DHPG) was low. This finding suggested an impaired NET activity which was further correlated with a genetic component as other family members suffered from similar symptoms. For the other ER-retained variant, A369P, no medical condition is indicated

in literature, however, the loss of function can only hint at faulty NET activity and concomitant failure in NE signalling (6, 97).

Apart from cardiovascular diseases, NET SNPs cause disruptions in arousal, stress response, emotional regulation and attention, with arising disorders like ADHD or depression. T283M, T283R, V382A and V245I set examples for variants which contribute to the pathogenesis of ADHD (98). For depression T182C has been postulated to be involved in its pathophysiology along with F528C, a gain-of-function mutant that was already mentioned above (96). Other psychiatric diseases like schizophrenia and Tourette syndrome were also investigated for NET variants and data do mention certain polymorphism like T182C, V1245I or G478S, yet, the results were not significant enough to share a direct link between disease and variant (99). Recently, T99I was detected to be overly present in athletes. Especially the change in myofibrillar structure seems to favour endurance athletes, suggesting a correlation between elite performance and the deficient NET functioning (100).

1.6.3 Genetics and Polymorphism of hGAT1

The SLC6A1 gene resides in chromosome 3q25.3 and encodes a protein of 599 amino acids. 45 point mutations for GAT1 are known up to this date, distributed across the transporter (6).

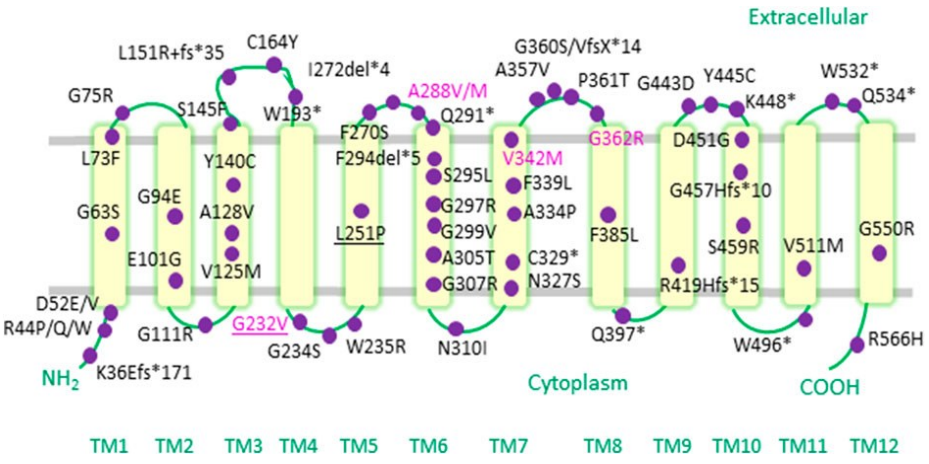

Figure 8. Topology of hGAT1 mutants with known SNPs.

The figure shows the known hGAT1 mutants in the 12-TMD-assembly as purple dots. Mutants recurring in the population are marked here in pink. The N- and C-termini are directed towards the cytoplasm and the mutants as usual are described in single-letter codes with the respective position of mutation defined in numbers.

In close proximity to the gate lay the variants G307R (TMD6b) and A334P in TM7, which do provide co-localization to the plasma membrane, nevertheless, they interfere with the structural arrangement of the transporter. Both are devoid of activity with an uptake below 5%, compared to A288V (TMD6) that shows a negligibly higher uptake capacity of 25%. Another group of variants, A128V (TM3) and G550R (TMD12), presents low levels of mature proteins along with G297R in TM6, suggesting the insufficiency of trafficking mechanism in this matter (101). Furthermore, the latter ones and P361T, another folding-deficient variant, are all ER-retained mutants devoid of any transporter activity. New studies revealed a new set of disease-variants that are closely related to the other ones in terms of pathogenesis: G443V and G443D, residing in EL5 (102). There is also a group of SNPs that possess a less trivial role in clinical disorders such as I405V, L415I and G533A (101). Several other mutants are known, which perturb trafficking, substrate binding and gating, however, those will not be discussed as it will only exceed the boundaries of this thesis.

1.6.4 Pathophysiology of hGAT1 variants

Polymorphisms of hGAT1 are widely known for their contribution to severe neurological and neurodevelopmental diseases. Autism, schizophrenia and a spectrum of epilepsy types are merely few affiliated with the little switch of a single nucleotide. Especially *de-novo*-mutants increase the risk of epilepsy and intellectual delay (6). The membrane-resident G307R is phenotypically expressed as myoclonic atonic epilepsy (MAE) and intellectual disabilities. A288V, A334P and G297R are also featured in a pool of missense mutations which implicates their involvement in MAE and intellectual disabilities. Severity of latter is wholly dependent on the mutant, ranging from mild retardation to highly delayed conditions (for instance in patients carrying G297R). As we can see, MAE is the most common type of epilepsy in these patients, suggesting that polymorphisms in the SLC6A1 gene follow a similar pattern of phenotype. Certainly though, few patients (less frequent) also fulfil the criteria for other types like generalized epilepsy and focal epilepsy (46, 48, 103). Another prominent example is G234S: This one is a genetically-transmitted and very unstable protein with occurrence in Lennox-Gastaut-syndrome (103). Similarly, P361T causes absence epilepsy and autistic disorder due to its misfolded nature. The clinical role of G550R was not investigated up to this

point, however, previous *in vitro* experiments suggest potential impact on neurodevelopmental and epileptic disorders (102).

One mutant in particular garnered a lot of attention after a two year old child suffered from intellectual delay and epilepsy. Results of genomic sequencing indicated a mutation in the hGAT1 gene: G443D. Further testing also concluded the transporter to be a loss-of-function variant retained within the ER. It lacks any reuptake activity (102). The sister mutant G443V shows similar characteristics, however, clinical studies miss to validate the pathophysiological implications (102).

1.7 Rejuvenating the ability of reuptake

Several methods have been tested in the past century to find a viable way of regaining transporter functionality. Especially those surrendering to their misfolded structure have been a topic of interest due to their clinical presentation in diseases. Correction of those defective proteins by means of chaperoning was a pivotal approach as the fundamental issue of folding and trafficking was tackled. We define three groups of chaperones: The more broadly acting chemical chaperones, the more selective pharmacochaperones and the intrinsic molecular chaperones, whereby latter shape the endogenous control system (79). Chemical chaperones as small molecules do not bind directly to proteins but much rather act as exogenous stabilizer. The process from raw protein to its final conformation is highly complex and calls for a decent amount of energy – owning to the hydrophobic segments of the transporter. Those would otherwise aggregate if the necessary milieu is not available and eventually surrender to degradation (2). Folding-deficient proteins succumb to exactly this step – they just cannot seem to reach their stable conformation.

Table 4. Members of chaperone groups.

Chemical chaperones	Pifithrin-μ, 4-PBA, DMSO, 17-DMAG, glycerol
Pharmacochaperones	Ibogaine, noribogaine, lumacaftor, tafamidis, bupropion
Molecular chaperones	Calnexin, calreticulin, HSP70, HSP90

The answer to the question why the alteration of one single amino acid has this vast of an effect is similar to searching for a needle in a haystack. Therefore, instead of solely understanding the problem, a solution is wanted. One very terrific finding was glycerol, a simple triol which is usually found as a hydrophilic solvent in pharmaceutical products. Glycerol was initiated on ΔF508, a cystic fibrosis transmembrane conductance regulator (CFTR) mutant known to cause cystic fibrosis, and successfully increased functional CFTR channels in the plasma membrane (104). The proposed mechanism of action is a stabilization of an intermediate that manages to escape degradation and afterwards enters maturation, ultimately refolding into a proper transporter. Dimethyl sulfoxide (DMSO) works in a similar manner by aiding to conquer the energy barrier from misfolded to a correctly folded assembly (2).

Other chemical chaperones include 4-PBA, 17-dimethylaminoethylamino-17-demethoxygeldanamycin (17-DMAG) and pifithrin-μ (6). 4-PBA is an FDA approved drug available in the US for the treatment of urea cycle disorders, that is believed to exhibit a pool of complex activities: protecting proteins from aggregation, relieving the rigid quality control, acting as a histone deacetylase inhibitor and reduce ER stress (105). Promising effects were also observed for CFTR ΔF508, mutants of human DAT, SERT, GAT1 as well as CRT in *in vitro* studies, which gives rise to hope for similar results in clinical trials (10, 106, 107). However, recent studies have abandoned the idea of aggregation prevention and added another role to the chaperone's already multifaceted nature: 4-PBA putatively minimizes protein synthesis by intervening in mRNA translation, that allows a reduction in protein load and thus, enables the ER to better manage the trapped misfolded proteins (108). As it seems, understanding the chaperone proves as a challenge – one, that calls for more research to fully comprehend its vast spectrum of pharmacological roles.

At least for now, no data denies 4-PBA's contribution to the quality control system just as pifithrin-μ and 17-DMAG of the same group (2, 10). Pifithrin-μ was reported to rescue DAT

variants as HSP70 modulator, while 17-DMAG increased the cell surface expression of synthetic SERT mutants as HSP90 inhibitor. Both failed to present dependable data for medical applications, though (109).

Table 5. Structures of chemical chaperones.

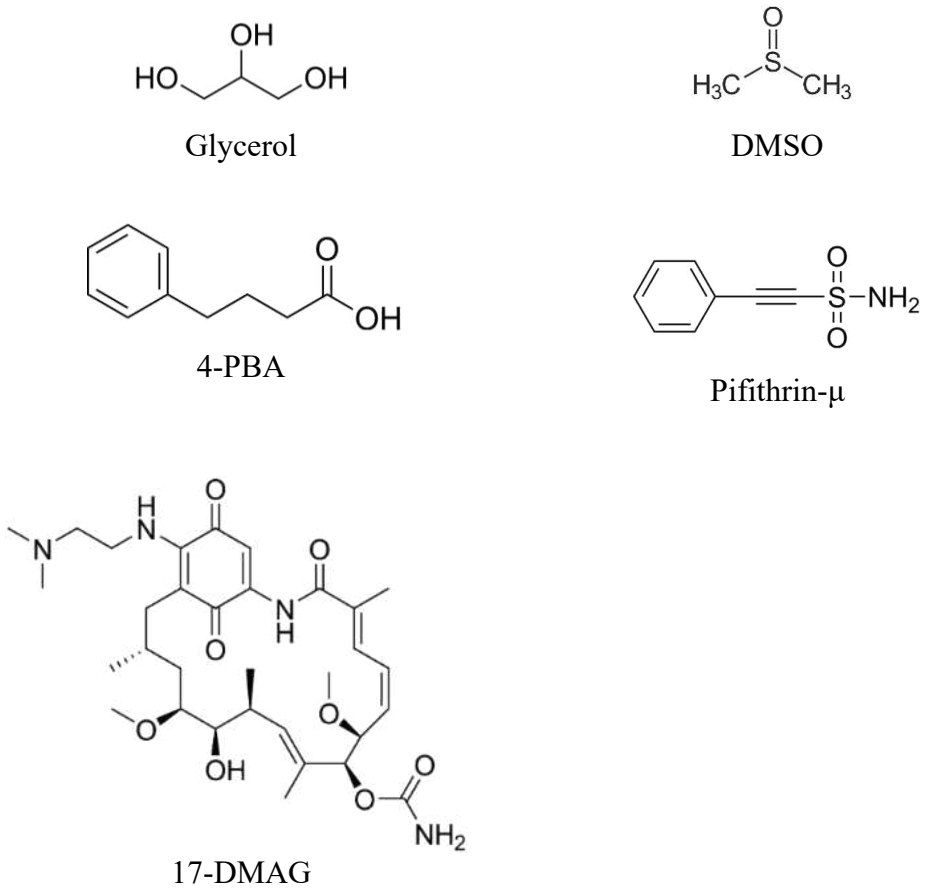

Unlike chemical chaperones, pharmacochaperones demonstrate a substrate specificity that allows them to bind directly to misfolded transporters, correct them and redirect the protein trajectory towards the cell membrane. To achieve this, the ligands have to be affine for an inward facing conformation of SLC6 members – which is challenging, considering that ligands usually bind an outward facing transporter (62, 108). Yet, noribogaine successfully recovered the functionality of misfolded DAT variants in *Drosophila melanogaster* (110). Additionally, treatment of SERT variants resulted in increased protein expression followed by higher level of cell surface expression (92, 107). Bupropion, a well-known NET and DAT inhibitor, also yielded remarkable results with an increase in mature and functional DAT mutants (8).

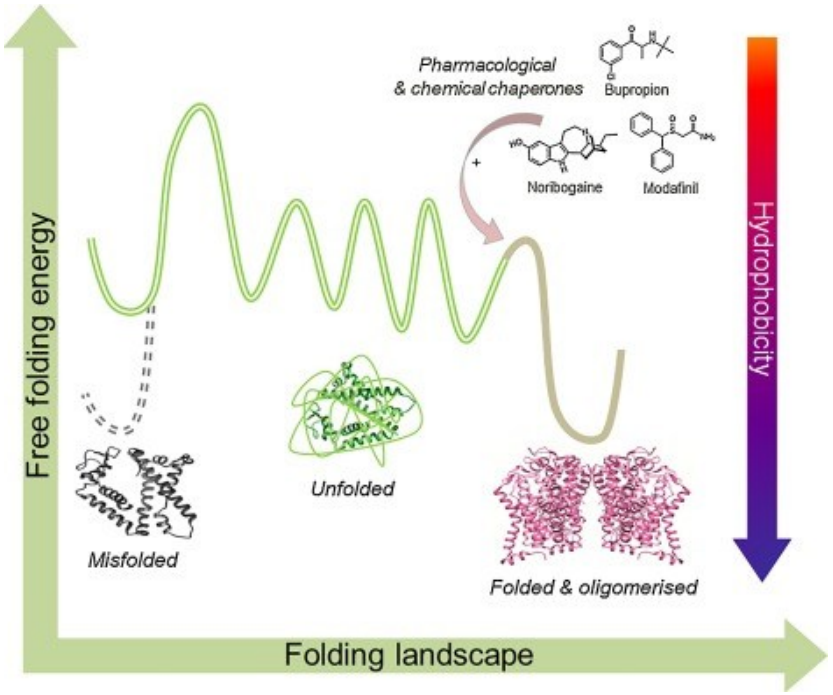

Figure 9. The folding landscape of SLC6 transporters, with regards to free folding energy.

The nascent polypeptide chain is energetically in an unstable state, thus it undergoes various states before it reaches its final stable and folded state with low free energy. In order for the unfolded state to not end up as misfolded, chaperones of various kinds can assist in folding. Two examples, as illustrated here, set bupropion, noribogaine and modafinil (2).

As for a GAT1 variant, treatment of transgenic flies with tiagabine increased transporter level in the plasma membrane, though the results were not as considerable compared to the others (109). Those outcomes implicate new candidates for possible therapeutic agents, that might address issues of deficient transporters and rescue them instead. Migalastat and Lumacaftor are two pharmacochaperones available on the market as treatment options for Fabry disease and ΔF508 generated cystic fibrosis (6). Another pharmaceutical already in clinical use is tafamidis, a synthetical drug that was specifically designed to suppress aggregate formation of mutated transthyretin and prevent the progression of amyloidosis (2).

Table 6. Structures of selected pharmacochaperones

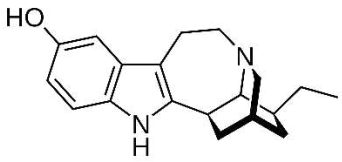 Noribogaine	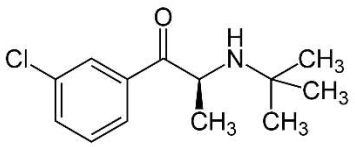 Bupropion
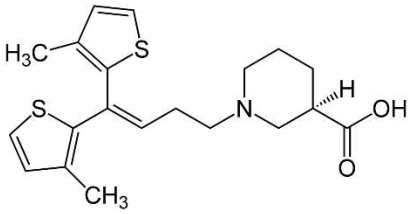 Tiagabine	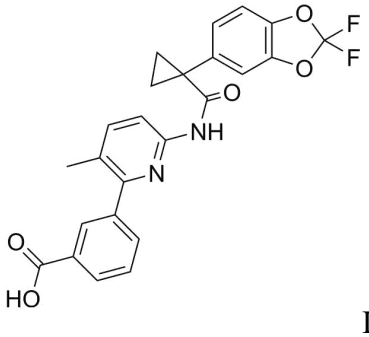 Lumacaftor
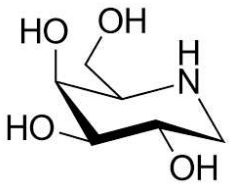 Migalastat	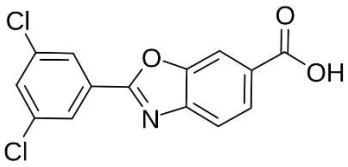 Tafamidis

From the collected data, we can reckon a strong potential for rescuing variants where research is either lacking or still in progress. In particular, studies on the NET variants A457P and A369P, as well as the GAT1 variants G445D and G445V are scarce (109). Considering the existing knowledge, there is a promising opportunity to deepen our understanding of these variants. By focusing our efforts on these areas, we could advance the knowledge for these variants and move forward.

2 Hypothesis

Genotypical changes can present in different manners: either no phenotypical expression at all, manifestation with little to no effects on quality of life, or the cause of what we call genetic disorders. Those differ on the location of abnormality, the type of abnormality, and the affected functionalities. Human GAT1 is solely located in the CNS, hence, mutants in this group are related to conditions such as autism, several types of epilepsy (e.g. absence epilepsy, focal epilepsy or Lennox-Gastaut syndrome), impaired cognitive delay, ADHD and more. In comparison, hNET is not merely found in the nervous system but also in the cardiovascular system, presenting disorders in case of mutants that are not limited to the nervous system alone. Schizophrenia, depression and tachycardia set just few examples that show the consequences when single nucleotides are switched. Especially when we notice the changes on a cellular level, we can see for few SNPs that the transporters already fail at cell surface expression. We accordingly plan our work on certain transporters devoid in the surface: G443D and G443V for hGAT1 mutants, A369P and A457P for hNET variants. Our question of interest remains how the mutants can be restored in their functionality. In this thesis, we put our main on hNET variants as research in this field is still very spare compared to hGAT1, where more data regarding mutant characteristics is available. For this sake we have limited our experiments for potential rescue methods of G443D and G443V and laid out more data for the hNET mutants A369P and A457P. To do so, we plan to apply chemical chaperones and pharmacochaperones as our mean of rescue mechanism. Based on evident studies, DAT and SERT mutants have been successfully expressed in the plasma membrane with the antidepressant Bupropion. Therefore, we assume that the priorly mentioned hGAT1 and hNET variants can be saved by employing a pool of compounds onto the mutants. We plan to analyse their rescue potential and check, if the compounds can be utilized for further research if they do inhabit promising effects.

3 Materials and Methods

3.1 Materials

3.1.1 Reagents

Cell culture medium, antibiotics, supplements, buffers and trypsin were acquired from Invitrogen. HEK293 cells were gained from Thermo Fisher (Massachusetts, USA) and authenticated by STR profiling at the medical University of Graz (Cell Culture Core Facility). Sodium dodecyl sulfate (SDS) was obtained from BioMol GmbH (Hamburg, Germany), the Complete™ protease inhibitor cocktail (PIC) and bovine serum albumin (BSA) by Roche Applied Science (Mannheim, Germany). Tris and scintillation mixture (Rotiszint® eco plus) were purchased from Carl Roth GmbH (Karlsruhe, Germany). As for the primary rabbit polyclonal anti green fluorescent protein (GFP) antibody we obtained it from Abcarn Plc (Cambridge, UK), the secondary goat anti-rabbit IgG antibody IDRye® was attained from LI-COR (Lincoln, Nebraska, USA). The radioligand ^{3}H-MPP+ (1-methyl-4-phenylpyridinium, 16.67 Ci/mmol) was from PerkinElmer Life Science (Waltham, MA, USA). [^{3}H]GABA+ was received from Revvity Inc. (Boston, USA). Trypan blue solution 0.4% along with Pifithrin-μ, 4-PBA, tiagabine and nisoxetine were purchased from Sigma-Aldrich (St. Louis, MO, USA). 17-DMAG was acquired from Cayman Chemical (Michigan, USA). The Ibidi® glass bottom chambers were from Ibidi (Gräfelfing, Germany). Solvents and common reagents (analytical or reagent grade) were obtained from standard commercial sources.

3.1.2 Media and Buffers

Preparation of buffers and media were done according to specific protocols. The cell media DMEM contained 584 mg/L glutamine and 4.5 g/L glucose and were supplemented with 10 % fetal bovine serum (FBS) and 100 U/ml of penicillin and 100 µg/ml of streptomycin, the addition of antibiotics was required to prevent contamination. The buffer phosphate buffered saline (PBS) was set at a pH level of 7.3 with a mix of NaCl 137 mM, KCl 2.7 mM, Na2HPO4x2H2O, 4.3 mM and KH2PO4 1.5 mM. For Krebs Hepes Buffer the same pH level

was attained after preparation with HEPES 10 mM, KCl 3 mM, NaCl 120 mM, CaCl2.2H2O 2mM, MgCl2.6H2O 2mM and Glucose monohydrate 2mM.

3.2 Methods

3.2.1 Mutagenesis

Mutants were generated by introducing single nucleotide changes to yellow-fluorescent-protein tagged hNET (YFP-hNET) and hGAT1 (YFP-hGAT1) as plasmid DNA templates. For the sake of this the QuikChange Lightning site-directed mutagenesis Kit was used. The desired mutant was inserted into the plasmid with primers of the same kit which harbour the desired mutant sequence.

Firstly, the DNA template was combined with two mutant-harbouring primers, each for one DNA strand. This step was followed by the addition of PfuTurbo DNA polymerase which replicated the DNA sequence along the paternal DNA. For segment two, the number of cycles depends on the type of mutagenesis conducted, in this case 12 cycles for a single nucleotide change. The product was treated with Dnp1 to break down the methylated parental DNA, leaving behind amplified mutant-containing DNA plasmids. The final products were either stored at -20°C or facilitated for transfection.

3.2.2 Cell Culture

All experiments were conducted in HEK293 cells (Human embryonic kidney 293 cells). HEK293 cells were incubated at 37°C in 5 % CO_2 humidified atmosphere in Dulbecco's modified Eagle's medium (DMEM), with the addition of FBS, penicillin and streptomycin. After reaching a confluency of approximately 80 %, they were carefully washed with PBS, which was removed right after, and detached with trypsin (0.25%). The HEK293 cells were incubated for another 5 minutes before they were suspended with DMEM. The cell suspension was placed in a centrifuge to separate the supernatant from the media+trypsin. The centrifuge was set at 1000 rpms for 5 minutes. Once done, media+trypsin were aspirated with only the

cells remaining. DMEM was added and the mixture suspended thoroughly. HEK293 cells were eventually re-cultured for the next experiments.

In case of cell counts, a reasonable number of cells needs to be available to facilitate them in experiments. The following table shows the required number on the day of seeding depending on the type and size of the dish.

Table 7. Number of cells required per dish size.

Dish for seeding	**Number of HEK293 cells per dish on day of seeding**
10cm petri dish	5×10^6
6cm petri dish	1.4×10^6
6-well plate	3×10^4
48-well plate	1.5×10^4

3.2.3 DNA-Transfection

For the transfection series, the cells from cell culture were further employed. HEK293 cells were seeded the day before transfection in either a 6cm or a 10 cm petri dish and left in the incubator at 37°C overnight. The upcoming day, a combination of Lipofectamine (LA) 2000 and OptiMEM was prepared and incubated at room temperature to be later added to the DNA and OptiMEM mixture.

Table 8. Volumes of OptiMEM and LA 2000 required for DNA transfection according to dish size.

	Volume for 6cm dish	**Volume for 10cm dish**
OptiMEM	0.5 ml	1.5 ml
LA 2000	15 µl	45 µl

Table 9. Plasmid volume for DNA transfection.

DNA reagent	Volume for 6cm dish (µl)	Volume for 10cm dish (µl)
hNET	6.7 µg / 1 µg/µl = 6.7	20
R121Q	6.7 µg / 2.3 µg/µl = 2.9	-
T283R	6.7 µg / 1.86 µg/µl = 3.6	-
N292T	6.7 µg / 0.75 µg/µl = 8.9	-
A369P	6.7 µg / 1.6 µg/µl = 4.2	12.5
A457P	6.7 µg / 1.058 µg/µl = 6.4	18.9

In regard to mutants R121Q, T283R and N292T we did not transfect the cells on 10cm petri dishes but only on 6cm dishes, hence only mentioned for latter dish size. Every dish was transfected with a respective transporter-encoding plasmid. Once joint, the transfection mix was kept to incubate at room temperature for 20 minutes. The solution was added onto the cells in a dropwise manner to prevent the cell from detaching. The DNA reagent remained at least 24 hours to ensure proper encoding and co-localization of the desired transporters. Later the cells were utilized for chaperoning, radioligand uptake assays, confocal microscopy and immunoblotting.

3.2.4 siRNA-Transfection

HEK293 cells were seeded in a 48-well plate the day before transfection. Per well a number of 1.5 x 10^5 cells was required. The well plate was coated twice with poly-D-lysine (PDL), with in-between incubation time of one hour followed by a washing step to improve cell attachment.

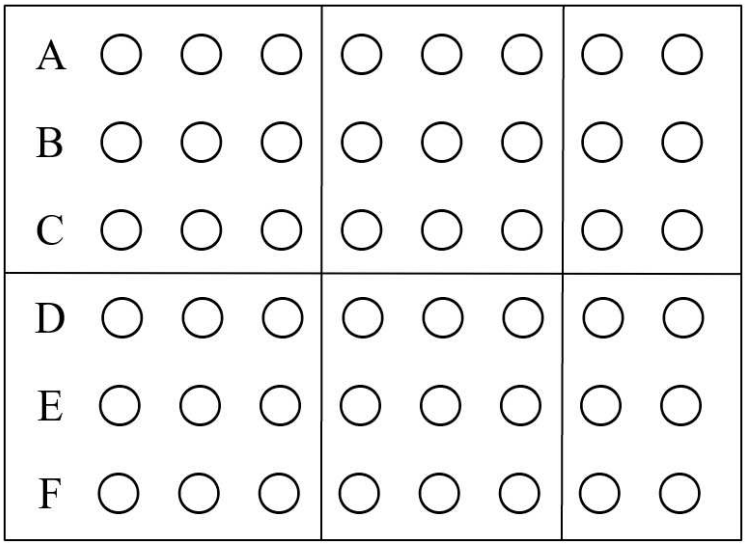

Figure 10. An illustration of 48-well-plate.

This figure depicts a 48-well-plate and shows how the corresponding rows and columns were used in uptake experiments. In regard to the rows, we had three each for WT and mutants. Each row was designated one for a blank (control), for small interfering RNA (siRNA) HSP70 and the last one for siRNA HSP90. For a certain viability of results, we chose three columns for each row. The last two columns served the purpose of cell counting after an uptake assay.

24 hours after seeding the cells to proliferate, a set of LA RNAiMAX with OptiMEM and two separate mixtures were prepared: one containing 5 pmol HSP70 RNA in OptiMEM and the other bearing 5 pmol HSP90 siRNA in the same media. Each siRNA was equal to 7 µl, however, we had two isoforms for each, hence we required 14 µl of siRNA in total per well. For control we treated them with scrambled siRNA which did not interfere with the mRNA at all.

LA RNAiMAX mix was left to incubate for 5 minutes, then combined in a 1:1 ratio with each siRNA mix and again left for 20 minutes of incubation. Meanwhile, cell media was replaced with fresh DMEM. The last step involved the addition of LA mixture to the respective rows. We let the dishes incubate for 48 hours in this condition before DNA transfection occurred. In regard to the required volumes, those are stated below in Table 10.

Table 10. Volumes used for siRNA transfection

	Volume per well
20 µM HSP70 siRNA	5pmol → V= 5pmol/20µM = 7 µl x 2 = 14 µl
20 µM HSP90 siRNA	5pmol → V= 5pmol/20µM = 7 µl x 2 = 14 µl
OptiMEM	15 µl
LA RNAiMAX	0.6 µl

3.2.5 Chaperone Treatments

The day after DNA transfection, the cells were treated with chemical chaperones or pharmacochaperones. The following table shows the final concentrations used for cell treatments.

Table 11. Concentration used for each chaperone.

Chaperone	**Concentration**
4-PBA	10 mM
17-DMAG	2 µM
Pifithrin	5 µM
Lumacaftor	5 µM
Glycerol	10 %
Venlafaxine	10 µM
Bupropion	50 µM

Cells were first removed from the petri dish and prepared accordingly to generate a cell suspension for seeding onto PDL-coated 48-well plates. The cells were resuspended in fresh media and treatment compounds. The necessary cell density per well was 10^5 cells, in the case of glycerol treatment, the cell number was increased to 1.5 x 10^5 cells per well (to compensate

for possible cell loss upon treatment). The plates were incubated at humidified atmosphere, at 37°C, in the incubator for 24 hours, for subsequent use in uptake assays on the following day.

3.2.6 Radiolabelled Uptake Assays

Uptake assays were carried out 24 hours *post* treatment. In case of chemical chaperones, the plates were washed once with Krebs-HEPES buffer (10 mM HEPES, 120 mM NaCl, 3 mM KCl, 2 mM $CaCl_2$, 2 mM $MgCl_2$, 2 mM Glucose monohydrate, pH 7.4), whereas pharmacochaperones were washed four times with Krebs-MES buffer (10 mM 2-(N-morpholino)-ethanesulfonic acid, pH 5.5, 120 mM NaCl, 3 mM KCl, 2 mM $CaCl_2$, 2 mM $MgCl_2$, and 2 mM glucose) and a fourth time with regular Krebs-HEPES buffer. Cells were incubated in the presence of either 10 µM nisoxetine (for hNET inhibition) or 10 µM tiagabine (for hGAT1 inhibition) for 10-15 minutes. These wells provided the data for non-specific uptake. After washing, the cells were incubated with either 50 nM ^{3}H-GABA or ^{3}H-MPP^+ at room temperature. The incubation time for ^{3}H-GABA uptake comprised 3 minutes, while for NET and mutants the radioligand was removed after 2 minutes with ice-cold Krebs-HEPES-Buffer. The last step was concluded with cell lysis *via* addition of 1% SDS. Uptake was quantified by liquid scintillation counting in a β-counter.

3.2.7 Confocal Laser Scanning Microscopy

This type of light microscopy was used to determine the exact localization of hNET, hGAT1 and mutants. A PDL-coated 6-well-plate was prepared with 3 x 10^4 HEK293 cells per well. For DNA transfection, we followed the same procedure except for slight adjustments in DNA concentration as we took 1.5 µg of plasmid and additionally 1.5 µg of Cyan-Fluorescent-Protein-Calnexin (CFP-CNX). This fluorescent marker highlights calnexin, which is, as we know, a resident protein in the ER. This enables us to detect proteins retained within the ER and even assists in assessing whether the treatment with chaperones has an effect on protein export or not. ER-marker and plasmid were diluted in 125 µl OptiMEM. For the LA 2000 mix we prepared 3.125 µl of LA 2000 in 125 µl OptiMEM per well. The rest went according to DNA-Transfection.

The day after, HEK293 were seeded onto an PDL-coated ibidi® glass bottom chamber with samples either receiving treatment or serving as controls. 24 hours later imaging was performed using a Zeiss LSM510 microscope with an argon laser at 30 milliwatts and a 63x oil immersion objective (Zeiss Plan-Neofluar). The cells were immersed in cell mask to display the plasma membrane.

Table 12. DNA volume for each condition in 6 well plate.

DNA	**Volume for 1.5 µg DNA (µl)**	**Volume for 1.5 µg CNX-CFP (µl)**
WT hNET	1.5	2.3
R121Q	0.7	2.3
T283R	0.8	2.3
N292T	2.0	2.3
A369P	0.9	2.3
A457P	1.4	2.3

3.2.8 Immunoblotting

HEK293 cells were utilized for lysate preparation either two days after DNA transfection or the day after treatment with desired compound. Cells were collected and centrifuged at 4°C for one hour with 1000 rcf (relative centrifugal force) in order to remove insoluble particles. The cells were taken into lysis buffer (containing 50 mM Tris·HCl, pH 8.0, 150 mM NaCl, 1% dodecylmaltoside, 1 mM ethylenediaminetetraacetic acid (EDTA)), and PIC to be then rotated for another hour at 4°C. Followingly the cells were centrifuged for 40 minutes at 4°C again. The supernatant, respectively the lysate, can be stored at -80°C and utilized for immunoblotting.

For further use we prepared aliquots of lysates with 20 µg protein content and let them run in an SDS-PAGE (sodium dodecyl sulfate polyacrylamide gel electrophoresis, 12 % monomer) western blot. The aliquots were applied to the gels and left running for an electrophoretic separation. The gels were then applied to polyvinylidene difluoride (PVDF) membranes with electrophoresis. The membranes were washed in Tris-buffered saline containing 0.1% Tween

20 (TBST) and afterwards blocked in a TBST solution containing 5% non-fat milk. The blocking solution was discarded after incubation time of one hour. This step was followed by an addition of TBST resolved primary rabbit polyclonal antibody from the GFP (1:5000 dilution) and Gβ (1:5000 dilution) type. These antibodies serve to stain the protein bands and mark them visible for detection later. The membranes were left at 4°C overnight for incubation. The primary antibodies were removed, and secondary goat anti-rabbit polyclonal antibodies were added in a dilution of 1:5000 to amplify the resolution of protein bands.

3.2.9 Statistical Data Analysis

Results were entered in an Excel sheet suitable for consequent analysis by GraphPad Prism 10 (Boston, USA). Data was assessed for normality and statistically calculated by one-way analysis of variance (ANOVA) with additional Dunnett´s t-test and Tukey´s post hoc t-tests. A p value < 0.05 represents a statistically significant difference. The experiments were done at least thrice (n=3) and carried out in triplicate in each experiment.

4 Results

4.1 Characterization of uptake capacity for WT hNET, A369P and A457P

The WT hNET is the main route for NE removal from the synaptic cleft. It hence eliminates signal transmission and enables release of NE anew once action potential hits. This is the way it goes under physiological conditions. However, mutants work otherwise and are represented in scenarios of phenotypical pathologies. We have compared the difference in activity of WT hNET with the SNPs A369P and A457P by conducting a radiolabelled reuptake assay of ^{3}H-MPP^{+}. Its affinity is similar to NE and allows us to detect the uptake with a β-scintillator. The experiments were done thrice with triplicates per experiment. As noticeable in Figure 11, the WT shows a regular activity level as physiologically present. In complete contrast, A369P has shown hardly to no uptake in this experiment. This outcome is concurrently observable for A457P as no ^{3}H-MPP^{+} uptake was recorded. The results for these two variants comply with our current knowledge that both transporters are unable of any uptake.

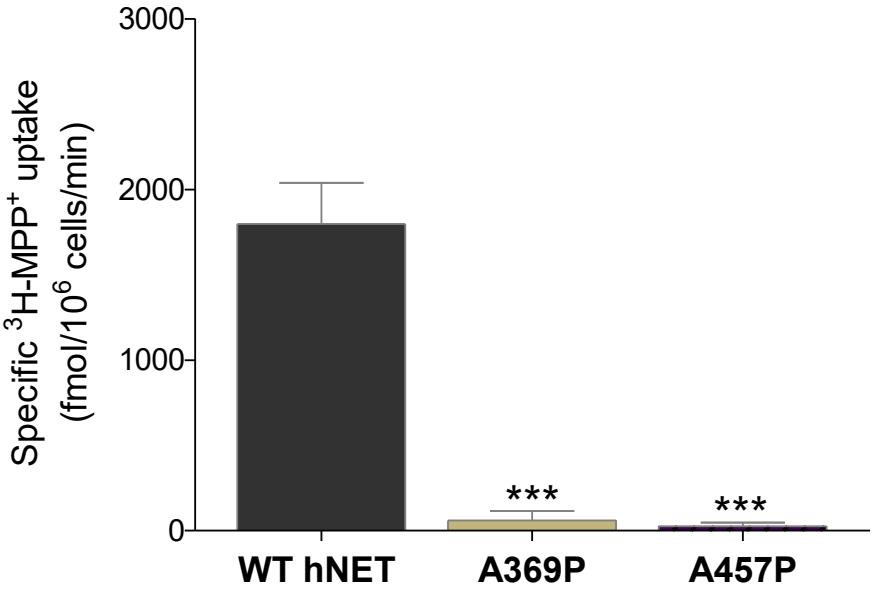

Figure 11. Uptake assay data for WT hNET and two variants thereof, A369P and A457P.

We prepared a number of 48-well plate dishes to measure the uptake capacity of WT hNET, A369P and A457P. HEK293 cells were transiently transfected with respective plasmid 24 hours prior to uptake assay. The following day, ^{3}H-MPP^{+} uptake was measured after 2 minutes incubation time. Non-specific uptake was determined after exposure to nisoxetine (10 µM) for around 15 minutes. As visible in the figure, ^{3}H-MPP^{+} uptake is detrimentally reduced for A369P and A457P compared to the regular transport rate. This confirms in a functional experiment that these transporters are void of transport ability (***; $p<0.001$, compared to WT hNET) The experiments were performed three times, each containing triplicates.

4.2 Determination of cellular localization for WT hNET and mutants

The uptake results make it evident that the transporters are reduced in their transporter activity. In order to see where the reason for this decrease lies, we have used the method of laser scanning microscopy. This way, we have tried to identify where the transporters are placed and if the transport rate may be correlated with their localization. Certain cell compartments were treated with markers and the N-termini of all transporters are tagged with YFP to pinpoint their

distribution. For the cell membrane we stained it with CellMask^{TM} Deep Red Plasma Membrane Stain, while calnexin (CNX) was applied to visualize the ER during confocal microscopy. We first took images for each marker separately for better orientation and overlayed them to illustrate possible differences between WT and mutants.

As for WT hNET, we see in Figure 12 a yellow lining of the membrane which appears if green and red light align. This confirms that YFP-tagged WT transporters are present on the surface. In order to visually demonstrate the difference in co-localization pattern for selected mutants compared to the misfolded variants, their microscopy results are included in this subchapter. When studying the co-localization for R121Q we see almost no difference to WT. Similarly, N292T merely shows a slight reduction in co-localization, which also complies with our results from the uptake assays. T283R, however, is underrepresented in the cell membrane as the overlayed pictures suggest. Instead, when comparing CNX and YFP-T283R images, we detect a higher transporter occurrence in the ER than on the cell surface. A finding that works well with the results acquired from the uptake assay (see

Figure ***11*** A). A greater difference of expression is visible for A369P and A457P in Figure 12: The plasma membrane shows hardly to none expression of both mutants, in fact, the transporters are present solely in the intracellular compartment. In reference to Figure 11 we can understand more clearly the absent NE transport if we bring the attained images into the picture: The overlay illustrations for both mutants capture well that A369P and A457P are retained in the intracellular compartment, to be exact, in the ER.

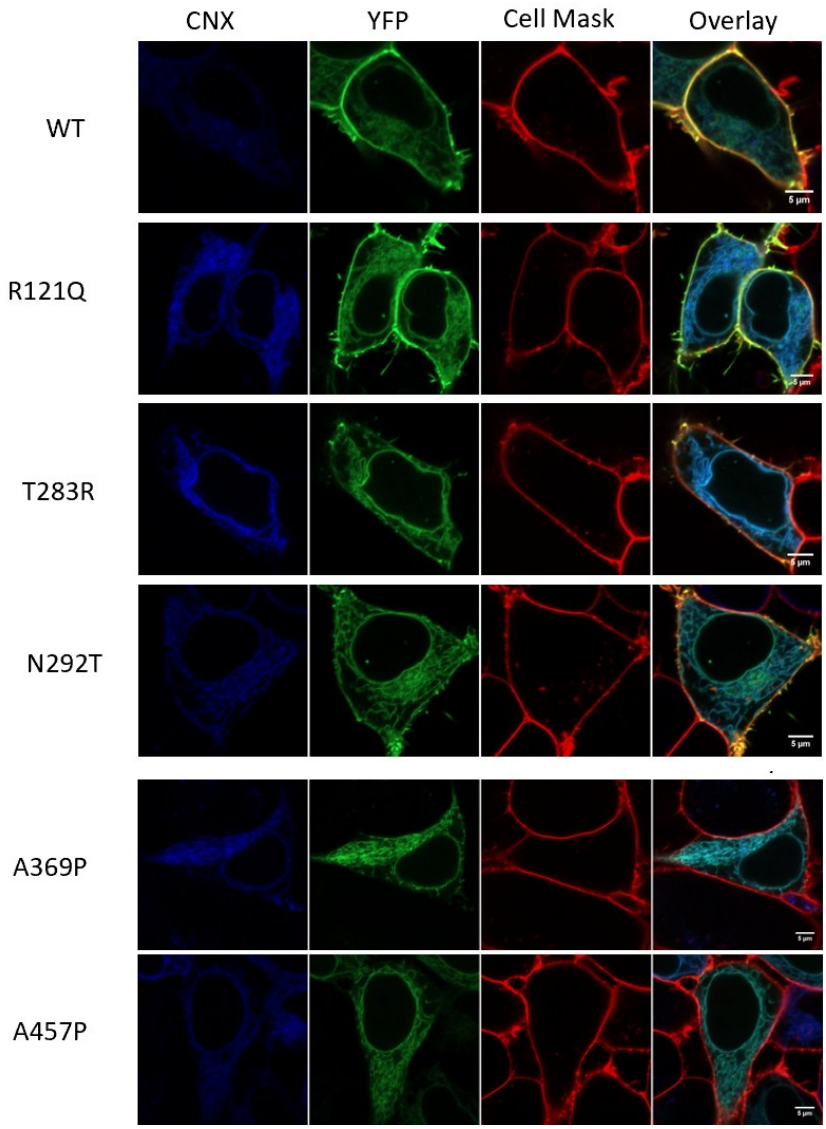

Figure 12. Images of WT and mutants from confocal microscopy.

WT hNET and mutants were tagged on their N-termini with yellow-fluorescent-protein (YFP). Images were taken 24 hours after transfection of HEK293 cells with respective transporter DNA. Calnexin (CNX) was used as a marker for the ER, while CellMask served to highlight the cell membrane. In A) we have WT hNET represented along with disease variants R121Q, T283R and N292T. All of them show a slight reduction in co-localization, whereas for A369P and A457P in B) the membrane is devoid of these diseases' variants.

4.3 Biochemical analysis of WT hNET and mutants

The radioligand uptake results reveals information on the functional activity of the transporters. Subsequently, we investigated their cell surface expression by immunoblotting. The WT hNET shows two bands, where the lower bands correspond to the ER resident proteins that are core-glycosylated. Upon core-glycosylation occurring in the ER, the WT is extensively glycosylated through the Golgi apparatus in order to be expressed in the plasma membrane as a functionally working transporter. These mature species represent the upper band (95 kDa). As displayed in Figure 13, the mature proteins are present for WT hNET, as well as its mutants R121Q, T283R and N292T, indicating that these proteins are expressed at the cell surface. The pathogenic variants A369P and A457P present no mature glycosylated species, but only core-glycosylated bands, suggestive of ER-retention (likely due to protein misfolding). Gß (at 34 kDa) served as a loading control.

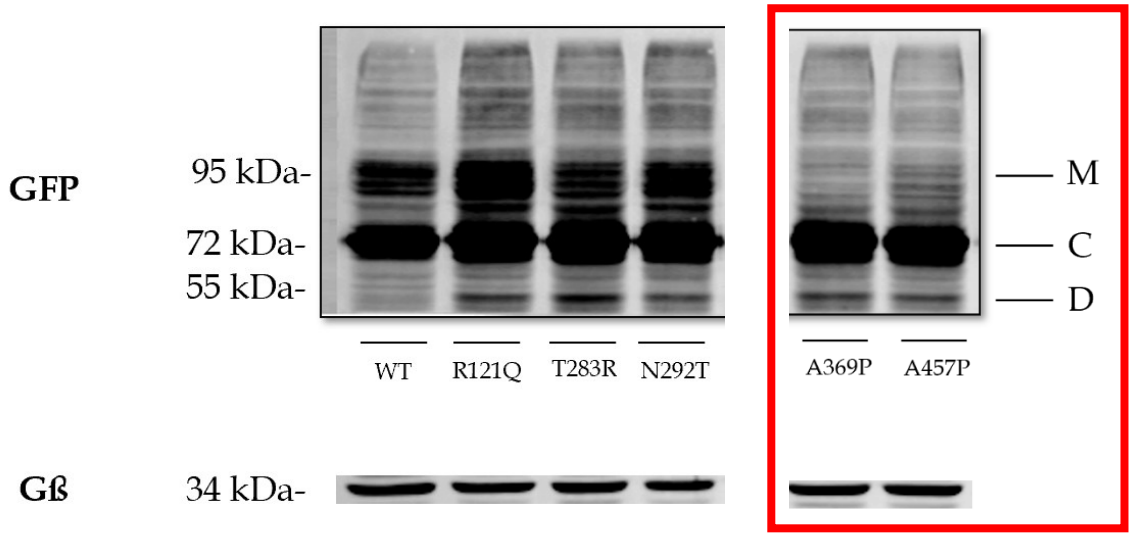

Figure 13. Biochemical assay of hNET and variants.

HEK293 cells were transfected with plasmids expressing the desired transporters. The bands portray various glycosylation patterns and allow for distinguishing between mature and immature protein species. GFP- and Gß-polyclonal antibodies were used to detect the bands. The maturity depends on the weight (represented here in kDa). 95 kDa (M) refers to the mature protein, 72 kDa (C) to the core-glycosylated protein and 55 kDa (D) to the de-glycosylated state.

4.4 Screening of misfolded hNET mutants for their response to a selection of chaperones

We have seen the diversity of disease variants present in a spectre of individuals. However, the ER-retained mutants are concerned with more severe effects on the quality of life than R121Q, T283R and N292T. Hence, within the scope of this thesis we have put our focus on the two misfolded transporters inhabiting A369P and A457. In the process, we relayed a variety of chaperones, trying out members from chemical chaperones as well as pharmacochaperones, and attempted to address the endogenous quality control directly by inhibiting HSP70 and HSP90. For latter, we have also tried this approach for hGAT1 mutants G443D and G443V as no data concerning this method is available. For the group of chemical chaperones, we examined the effects of 4-PBA, pifithrin-μ and 17-DMAG on hNET mutants. As previously elucidated, 4-PBA alleviates ER stress and potentially restore activity of heavily misfolded CRT mutants (107). Therefore, we have employed the chemical chaperone with the same idea that a rescue might be enabled. Along with 4-PBA, we have assessed the rescue potential of HSP inhibitors pifithrin-μ and 17-DMAG on the hNET variants (65). Pifithrin-μ operates by directly disrupting HSP70 activity and has restored functionally diminished DAT mutants this way(65). For 17-DMAG the mechanism of action involves blocking ATP hydrolysis of HSP90 which henceforth deactivates the chaperone and allows proteins to be freed from the rigid quality control (111). This compound exhibited this effect successfully on misfolded SERT mutants, therefore, this compound was also of interest for us to exhibit on A369P and A457P (65). Glycerol is another prominent chaperone as it stabilizes immature proteins during folding and worked wonders on hCRT mutants ΔF508. Because these molecules have demonstrated promising results we have employed them on the ER-retained hNET mutants in order to judge their rescue potential in this matter.

Among the group of pharmacochaperones we have engaged Lumacaftor and two antidepressants, Venlafaxine and Bupropion. Lumacaftor is a drug already on the market for the treatment of the CFTR mutant ΔF508, which is why it was of interest to us for application on A369P and A457P. Just as attractive was Bupropion that has proven effective in treatment of several DAT disease variants (8, 65). In case of venlafaxine, we know that the antidepressant works exactly the way it is supposed to: inhibition of NET. However, we still planned to check whether possible restoration of A369P and A457P could be taken into consideration, especially after an increase of surface expression for DAT mutants following a treatment with bupropion

was observed (8). We were wondering if venlafaxine might serve as an allosteric modulator for those two disease variants and thus assessed this compound's rescue potential for those.

Lastly, we tried to directly silence the endogenous chaperones HSP70 and HSP90 by inducing genetic knockdown. We introduced siRNA for each HSP to our HEK293 cells and temporarily shut down their expression. This way we planned to cease the quality control system and release the misfolded proteins from degradation. In this case we applied the method not only on hNET mutants but also on the hGAT1 disease variants G443D and G443V.

4.4.1 Employing chaperones on hNET variants

We tested the compounds 4-PBA, 17-DMAG, pifithrin and Lumacaftor on our mutants to see if they act on A369P and A457P. WT HNET has shown an increased uptake rate after treatment with HSP70 inhibitor 4-PBA as well as HSP90 blocker 17-DMAG, whereas the addition of pifithrin-μ did not do much. Lumacaftor also slightly increased the WT activity, but it is of no significance. Unfortunately, we did not notice a remarkable effect on transport rate for the mutants. After treatment, the cells expressing mutated transporter were still devoid of noteworthy uptake activity. For A369P, we see a slight increase in uptake compared to the other compounds, however, the difference is below 5% and hence of no significance. Same applies for A457P: The modest increase of ^{3}H-MPP^{+} after exposure to 4-PBA and 17-DMAG is of no relevance. The pharmacochaperones Lumacaftor could not restore the functionality either as opposed to our expectations. Glycerol, though, shows an increased A369P and A457P activity, suggesting a potential protein rescue. In regard to this compound, we will elucidate it in a separate chapter with separate experiments.

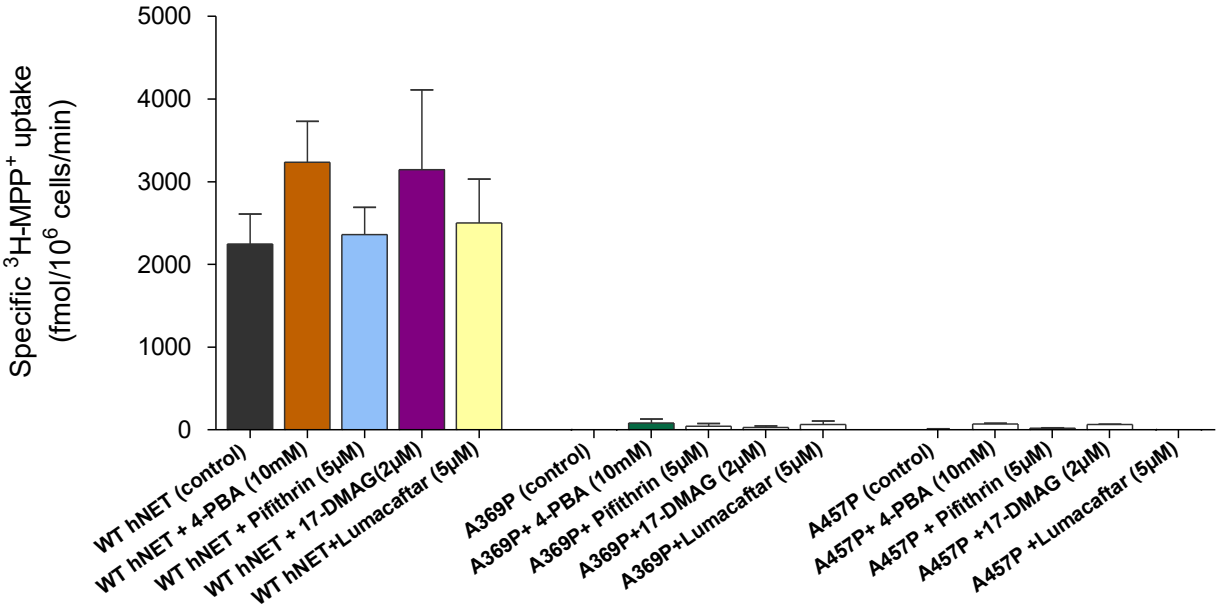

Figure 14. Rescue potential of A369P and A457P after treatment with chemical chaperones and lumacaftor.

HEK293 cells were transiently transfected with transporter plasmid in a 48-well plate and left for 24 hours before treatment. We exposed the cells to 4 different compounds in different concentration: 10 mM 4-PBA, 2 µM 17-DMAG, 5 µM pifithrin-µ and 5 µM lumacaftor. The well plate was left overnight for incubation and extensively washed afterwards. We added 10 µM nisoxetine to three columns in order to prevent non-specific uptake and left for an incubation time of around 15 minutes. Right after we added 50nM ^{3}H-MPP$^+$ to measure the specific uptake and removed it 3 minutes later. To contrast the non-specific uptake columns, we had three other columns to quantify non-specific and specific ^{3}H-MPP$^+$ uptake simultaneously. Treatment of WT with 4-PBA and 17-DMAG resulted in modest increase of substrate uptake and no increase after treatment with the other chaperones. We could not observe such increase in ^{3}H-MPP$^+$ uptake for the mutants. The data sets are statistically compared to the WT control by one way ANOVA, followed by Tukey's post hoc tests ($p>0.05$, compared to WT hNET). Data were obtained from four experiments, done int triplets.

4.4.2 Evaluating the pharmacochaperone potential of antidepressant drugs on hNET, A369P and A457P

In addition to the chemical chaperones and lumacaftor we utilized the antidepressants venlafaxine and bupropion, the latter already proven to be effective in another monoamine transporter. In hope that these two pharmaceutical drugs demonstrate their pharmacochaperoning abilities on the ER-retained mutants, we transfected the cells according to the protocol described above and set two conditions 24 hours after transfection: one well plate required the treatment with 50µM bupropion, and the other well plate got 10µM venlafaxine. Except for the treatment option, we concluded the experiment the same way as elucidated in the previous subchapter. As depicted in

Figure ***15*** A, data indicate a possible increase in transport activity by the WT hNET, but a similar result was attained neither for A369P nor for A457P. Regrettably, treatment with venlafaxine did not remedy the issue of failed substrate transport either (see

Figure ***15*** B). Venlafaxine acted in an analogous way on WT hNET with an increase, yet it has failed to rescue A369P and A457P. However, even if the results do not speak for an effect on both mutants, we still cannot exclude a possible increase of activity for other misfolded mutants of the same group.

A

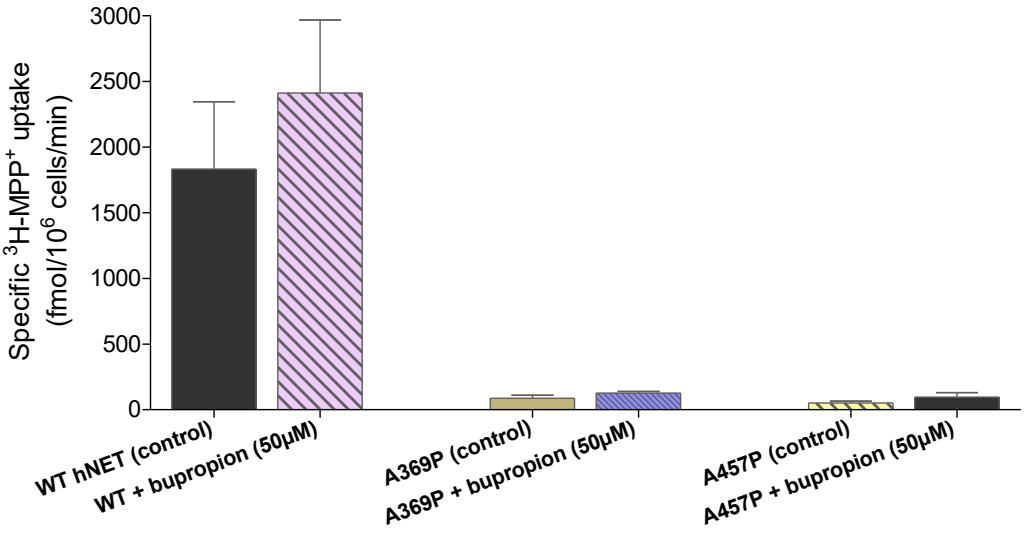

B

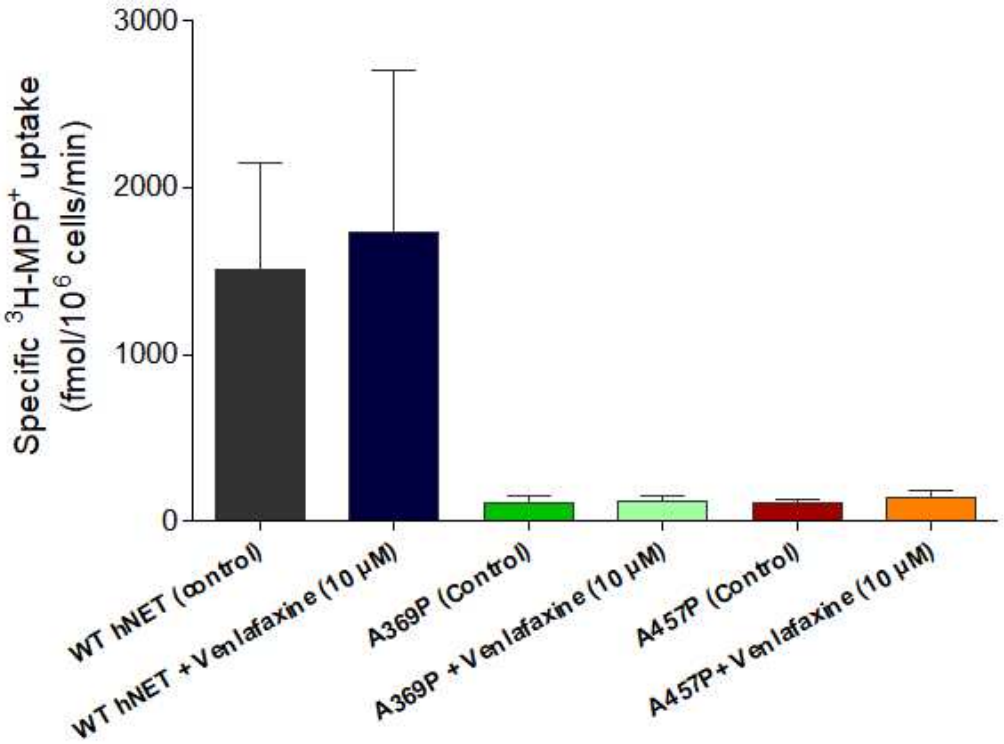

Figure 15. Results after treatment of WT hNET, A369P and A457P with putative pharmacochaperones.

HEK293 cells were transiently transfected with desired plasmid prior to treatment. The cells were subsequently treated with either bupropion (50 µM) or venlafaxine (10 µM). 24 hours later we washed the dishes with Krebs-MES-buffer to detach remaining compounds from WT and mutants, then initiated a radiolabelled uptake assay. We prepared columns for specific uptake after removal of nisoxetine (10 µM), and columns quantifying non-specific as well as specific uptake. Graph **A** shows the results for

^{3}H-MPP^{+} (50nM) uptake, measured 24 hours *post* treatment with bupropion. The data indicate a possible increase in transport activity by the WT hNET, but no response by A369P or A457P ($p>0.05$, compared to untreated controls). For **B.** ^{3}H-MPP^{+} uptake was determined 24 hours after venlafaxine treatment. For this condition, venlafaxine slightly increased transport rate for WT, regardless of that no such increase was detected for A369P or A457P.). The data sets are statistically compared to the WT control by one way ANOVA, followed by Tukey's post hoc tests ($p>0.05$, compared to untreated controls). The data was acquired in three independent experiments, each done in triplicates.

4.4.3 Response of hNET mutants and hGAT1 mutants after suppression of endogenous chaperones

Following the failed treatment of HSP70 and HSP90 with chemical chaperones, we tried to silence the quality control directly. For this reason, we applied siRNA for each chaperone. The RNA binds the respective mRNA sequence and triggers degradation of the target RNA sequence. We tried this method on A369P, A457P and on the hGAT1 mutants G443D and G443V. With respect to WT hNET, there was a decrease after silencing of HSP70, however, it did not apply either for A369P or A457P. The slight increase of A457P after HSP70 inhibition is non-noteworthy, for A369P the change was negligible. They also remained untouched after HSP90 inhibition, suggesting that the transporters cannot be rescued after relieving the control system. For hGAT1, we have in increased transport rate post treatment for the WT. If we see the results for the mutants, the increase for G443D is limited to 2-3% after treatment with both types of siRNA compared to its control.

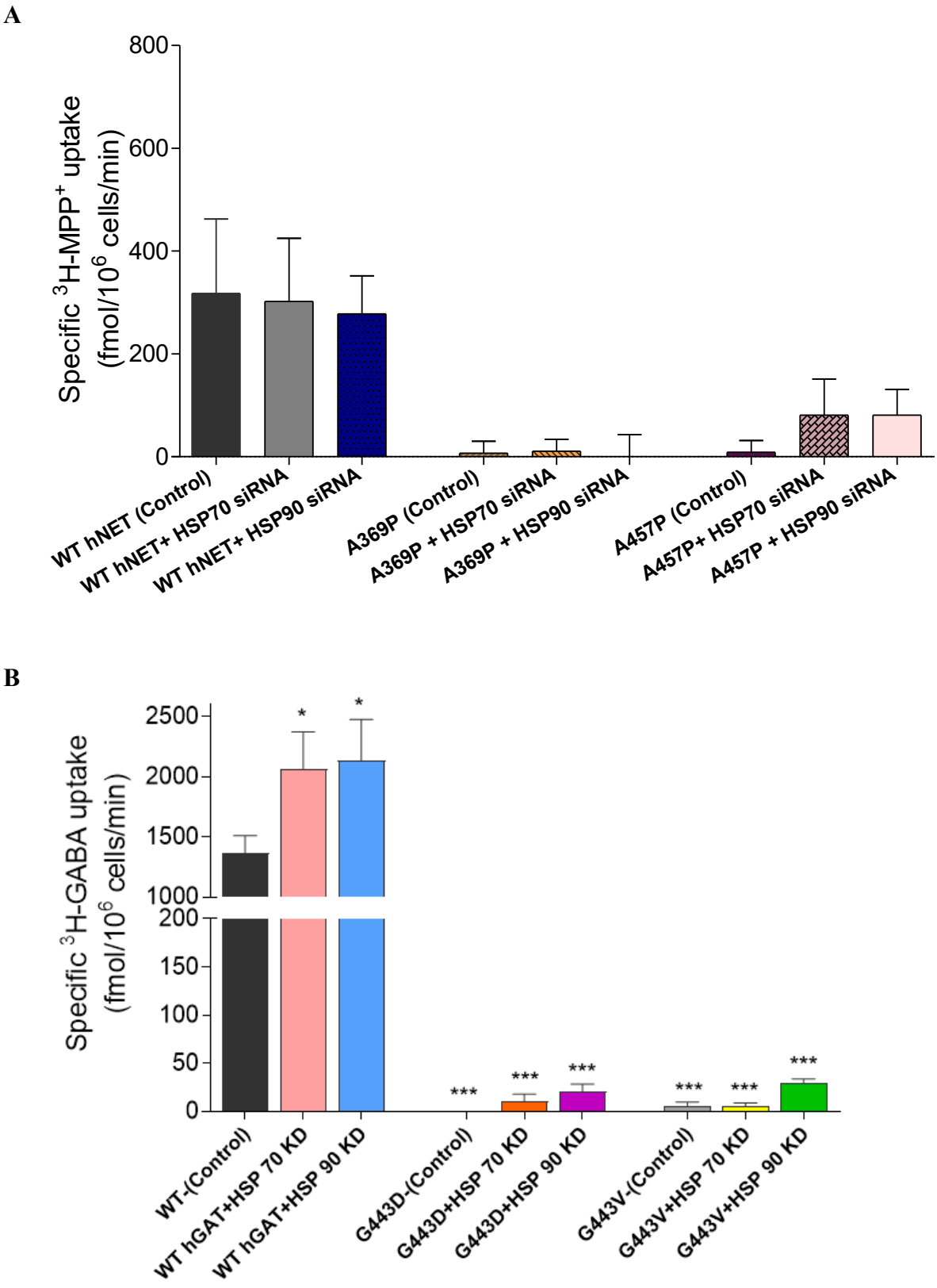

Figure 16. Reuptake activity after suppression of HSP70 and HSP90.

HEK293 cells were transfected with two isoforms of HSP70 and HSP90 and left for a duration of 48 hours in the incubator. The cells were transfected with required plasmid in order to the measure uptake

the day after. Specific uptake for A) was done with ^{3}H-MPP^{+} (50nM), whereas B) shows the results with ^{3}H-GABA (50nM). Non-specific uptake was done with nisoxetine (10 μM) for **A** and with tiagabine (10 μM) for B). For graph A) we see a slight decrease in transport for WT after treatment with siRNA HSP70 and siRNA HSP90. The transport rate for A369P and A457P after treatment with both types of siRNA has no significant effect compared to WT hNET. In graph **B** WT hGAT1 show an increase in transport activity after treatment with siRNA HSP70 and siRNA HSP90, however, this is not the case for mutants G443D and G443V. If the effects for treatment of G443D is compared to G443D control, there is a mere increase of 2-3%, for G443V post treatment compared to G443V control shows 5-6%. If compared to WT hGAT1, the increase in activity is of no significance The data sets are statistically compared to the WT control by one way ANOVA, followed by Tukey's post hoc tests ($p>0.05$; *, $p<0.05$; **, $p<0.01$; ***, $p<0.001$). The results were gained in three independent experiments with triplicates for each.

4.4.4 Rescue of hNET variants following glycerol treatment

Glycerol has proven to be efficient in facilitating protein folding and providing protein stability during folding processes. Especially after the successful story of ΔF508 rescue gave hope to the idea that this alcoholic molecule might remedy the misfolded happenings of A369P and A457P. We used a concentration of 10%, as previous experiments suggested for best outcome, and applied it onto HEK293 cells. The following day we obtained our results with a remarkable increase for both mutants. In Figure 17 we see that Glycerol has no effect on WT, but it looks otherwise for the mutants as uptake activity was restored with significance. This implies that A369P and A457P may regain transporter activity if exposed to glycerol in 10% concentration.

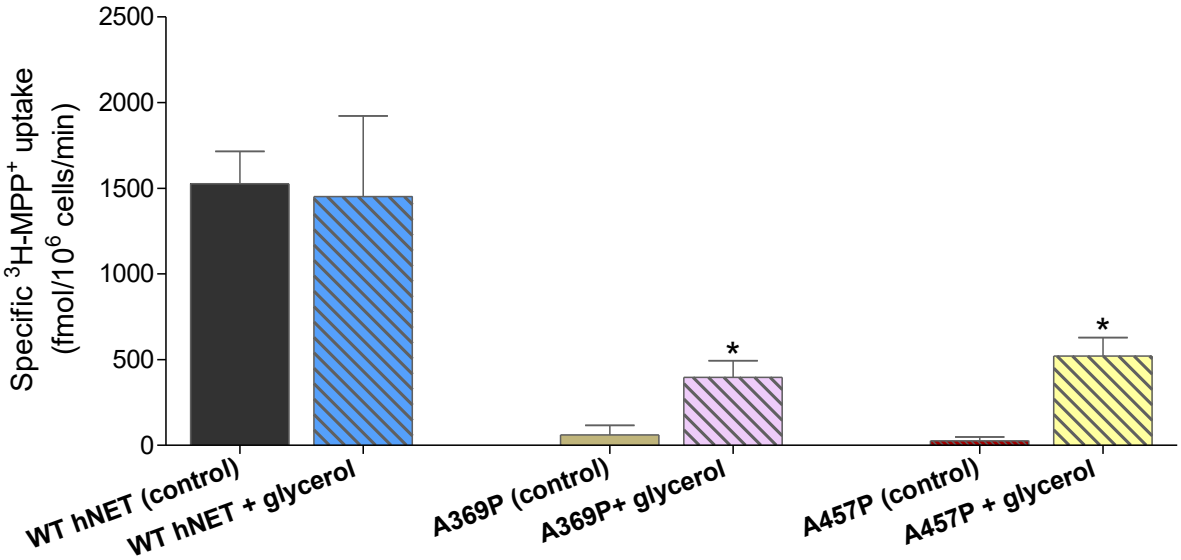

Figure 17. Rescue of A369P and A457P after glycerol treatment.

Glycerol 10% was tested upon DNA transfection of HEK293 cells. We first seeded them in a 48-well plate and transfected the cells the day after. After plasmid transfection, we waited 24 hours and applied glycerol 10% upon the transfected HEK293 cells. The day after the cells were extensively cleared off remaining chaperone and readied for uptake. Specific uptake of ^{3}H-MPP^{+} (50nM) was measured, while nn-specific uptake was done with nisoxetine (10 µM). We observed a significant elevation of transport rate for both mutants compared to control. This speaks for a successful rescue of mutant activity. The data sets are statistically compared to the untreated controls by one way ANOVA, followed by Tukey's post hoc tests (*, $p<0.05$). Experiments were done thrice separately with triplicates for each experiment.

4.5 Expression of rescued hNET mutants in a biochemical assay

The uptake assays for A369P and A457P demonstrated an increased transport rate after glycerol treatment. Hence, we desired to check whether the increase in transport arose from an increase in co-localization of transporter. We ought to answer this question with an SDS-page immunoblot, where we assess the rate of mature, core-glycosylated and de-glycosylated protein. This way we can identify which state is more prominent and if glycerol affected the presence of any protein state. As elucidated in Materials and Methods we have three bands with respective molecular weight of interest: the mature protein present at 95 kDa, the core-glycosylated state referred to 72 kDa and the de-glycosylated, non-functional protein band at 55 kDa. The Gß band here as well serves as a housekeeping band assuring reliability of experiments. It is shown in Figure 18 that WT is regularly expressing 95 kDa proteins bands

along with 72 kDa core-glycosylated bands, indicating presence of ER-resident proteins. When compared to the blots for A369P, we hardly see any band present at 95 kDa both for control and post treatment. The band at 72 kDa is darker confirming that the proteins still reside in the ER. However, as opposed to the control band, no de-glycosylated protein bands are visible. A similar observation was done for A457P: We see a slight but non-significant increase of mature protein. Interestingly enough, the de-glycosylated bands are missing, indicating at the sole presence of the core-glycosylated band. These results suggest that the degradation of core-glycosylated protein is decreased after glycerol treatment.

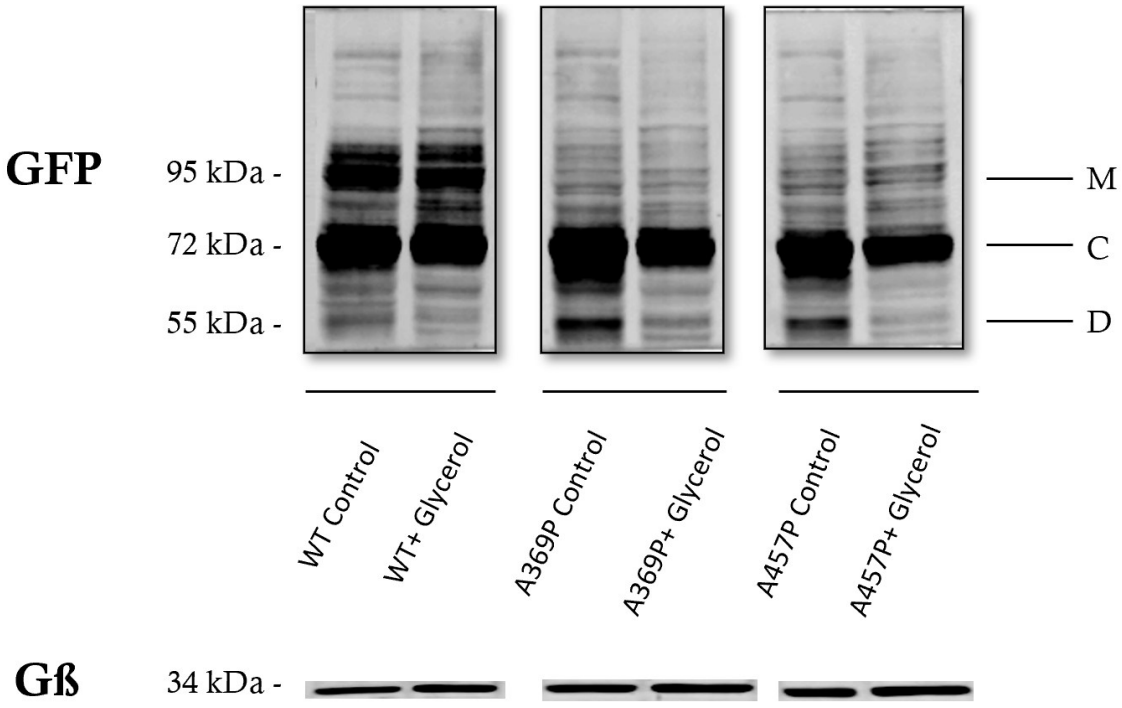

Figure 18. Immunoblots of WT hNET in comparison to the A369P and A457P variants.

An SDS-PAGE western blot was done for WT hNET, A369P and A457P. We detected the protein bands with respective polyclonal antibodies, GFP-antibodies for GFP bands (between 55 kDa und 95 kDa) and Gß-antibodies for the housekeeping gene at 34 kDa. The 72 kDa (C) demonstrates the core-glycosylated protein band while 95 kDa (M) represents the mature band. The visible bands at 55 kDa bands (D) display the de-glycosylated state. WT shows a regular pattern of mature protein, whereas those bands are missing for A369P and A457P after treatment. The expression of core-glycosylated is the case for all, for WT just as much as for the mutants. Regarding the immature de-glycosylated band, those are not present either for WT control or WT post treatment, however they are observed for A369P and A457P control.

5 Discussion

Folding- deficient- mutants are of great concern in the medical field because the arising phenotypical pathologies are based on molecular, respectively genetical changes that cannot be treated in a trivial manner. The SLC6 members hGAT1 and hNET possess a group of variants that are visible as diseases which comprise a patient's life quality. In case of hGAT1, associated disease variants are related especially to different kinds of epilepsy, a treatable condition usually but not anymore if the base of disease is not addressed correctly (112). The transporter is responsible for around 75% of GABA clearance, making clear the detrimental role of loss-of-function-mutants (49). hNET is not of less importance either, especially since it is present in the cardiovascular system just as much as in the nervous system. The transporter takes up approximately 80% of NE and therefore plays a major role in transmission modulation as well (23). We can suspect that mutants for this transporter are involved in an even broader spectre of diseases due to its ubiquity, encompassing Tourette syndrome to orthostatic intolerance (97). For a reuptake of neurotransmitter to succeed, though, expression of functional transporters in the plasma surface is required – if not applicable, the transport will diminish. SLC6 members present a great deal of mutants with diminished uptake activity due to misfolded transporters which did seem to reach the cell membrane. A proper tertiary structure is essential for an unproblematic export towards the cell surface, yet certain SNPs change the moiety of a protein to disable the transporter. We saw such cases for DAT and CRT mutants, where individuals suffer from early-onset Parkinson or mental retardation for the reason of failed transporter export (112).

As shown in the figures before, certain hNET transporter mutants still produce a neurotransmitter uptake, less compared to the physiological level but still enough to function well enough in a living being. On the contrary, A369P and A457P (latter in particular) bring down the modulation functionality to almost zero. In order to remedy the misfolded states, we have employed a pool of chaperones onto the ER-retained mutants and checked for potential effects on uptake. Chemical chaperones have worked before on other MAT (DAT and SERT), which is why we wanted to see if they act on A369P and A457P just as well as in the other mutant models. 4-PBA and 17-DMAG interact with endogenous chaperones HSP70 and HSP90 and relieve the protein control machinery (96, 107). It was one approach for us to keep the misfolded proteins from degradation and possibly enhance co-localization as a consequence. The results however implied no change in activity for the mutants as they were still devoid of transport activity. The other chemical chaperone pifithrin-μ has shown promising

results in treatment of misfolded DAT mutants, therefore we applied it on our folding-deficient hNET variants. After treatment we declared the same results with no improvement on uptake. Even if those chaperones revealed promising potential on other MAT variants, no such outcome could be registered in hNET models.

As a result, we opted for an alternative path by directly inhibiting the endogenous chaperones HSP70 and HSP90. Both of them ensure proper protein stabilisation and folding for subsequent export, however, in case of problematic nascent proteins, they mediate towards ERAD. The chaperones are rigorous with protein control and do not leave room for slightly changed proteins to survive. Thus, we directly silenced their action and attempted to encourage delivery of misfolded proteins which might be still efficacious. This method was applied on both hNET variants and hGAT1 mutants G443D and G443V, as no data for this approach on hGAT1 is available. By means of siRNA transfection we stopped any mRNA translation into HSP70 and HSP90 proteins and subsequently silenced their activity altogether. Our idea was not approved by hNET, the mutants revealed no significant increase after HSP90 suppression and the results for siRNA treatment of HSP70 provided no change at all. We found comparable results for the hGAT1 mutants, even though inactivation of the endogenous chaperones revealed an increased uptake activity of 2-5% for the mutants compared to their respective control. When brought into relation with the WT hGAT1, these effects are not of notable relevance. This might signal that HSP70 and HSP90 are not involved in the molecular pathology of these folding-deficient variants which requires us to approach the mutants from another perspective, possibly more selectively e.g. with pharmacochaperones.

Consequently, we moved on to pharmacochaperones, which act more selective on transporter compared to chemical chaperones. We initiated our attempts with Lumacaftor, a market drug that functions as a chaperone of the ΔF508 CFTR-mutant. It successfully aids in proper protein folding and increases the expression of stable CFTR (113). In our attempt to treat the misfolded hNET, they did not react to the compound as well as the ΔF508 mutant. The uptake assay did not reveal a potential effect, but the cells were still lacking functional transporter.

We then deployed bupropion, an antidepressant bearing a hidden skill that enabled a conformational reconstitution of misfolded DAT protein followed by increased mature states of same proteins. The mechanism of action is based on stabilization of an inward-open state that increased the DAT mutant co-localization (8). Our hypothesis was that the hNET mutants may be rescued in an analogous manner. We applied the compound on hNET and the results

for WT revealed an increased activity, suggesting possible assistance for surface expression. However, we could not detect comparable effects for both A369P and A457P. It is possible, though, that bupropion might function as a chaperone for other hNET mutants which are not as heavily misfolded as the ER-retained ones. Similarly, venlafaxine was applied to see if the antidepressant might also act as a stabilizer for misfolded proteins by trapping the transporter in an inward-open state and aid transporter expression. The uptake assay did reveal an increased transport activity for WT, but neither for A369P or A457P. Still, we cannot rule out the possibility that venlafaxine might work on other hNET mutants which are not completely void of transport. Further experiments are therefore required to validate this idea and investigate the rescue potential for the not as significantly misfolded transporter compared to A369P and A457P.

In our studies, the misfolded hNET mutants were exposed to 10% glycerol, a chemical chaperone previously shown to enhance the surface expression of the CFTR mutant ΔF508 (104). As illustrated in Figure 17, glycerol rescued A369P and A457P, shown by an increase in their functional uptake activity upon a 24h treatment. However, these mutants did not respond to any other chemical or pharmacological chaperone treatments used in our drug screening experiments. Glycerol likely acts by preventing the hydrophobic moieties of the protein from aggregating and hence, enables proper folding of mutant transporters and their delivery to the pertinent site of action i.e., the plasma membrane. In order to assess whether treatment with this chemical chaperone improved the localization of the mutants (i.e. improved their cell surface expression), we utilized biochemical assays (i.e. immunoblotting). In contrast to the uptake results, the effects could not be reliably detected and require further optimization (e.g. to reduce cell loss and possible cytotoxic effects of DNA transfections and treatments, using coated cell culture ware, examining the thermostability of the proteins). The preliminary data show that the mature bands for A369P and A457P after treatment with glycerol were not significantly improved in comparison to the control (without treatment). There is however an absence of the de-glycosylated band, which suggests that the chaperone prevents degradation into the functionless polypeptide chains.

Gaining knowledge in this field of research is substantial, to not solely better understand the molecular basis of diseases, but also to offer effective therapeutic strategies to a patient. Therefore, finding working compounds in terms of chaperone potential are essential to rescue loss-of-function variants. Other papers have published a pool of acting molecules (e.g. 4-PBA, noribogaine/ibogaine, bupropion *et cetera*) that exhibit the necessary clinical application (6, 8,

107, 112). Especially relevant are pharmaceutical drugs, which are already on the market, as enough data regarding their possible adverse effects, therapeutic index and more, are already available. Finding out that a compound like bupropion has displayed promising effects as a chaperone means that related molecules might also exhibit similar or enhanced rescue properties. We here found that the functional rescue of transporter disease variants is not a straightforward path, but even minor increments in each such study can provide crucial information. For instance, bupropion and venlafaxine might potentially benefit other hNET variants, not investigated in the scope of the present thesis. Our data reveals the hidden chaperone potential in diverse small molecules. Glycerol, for example, inhabits versatile properties and our preliminary data revealed a broad spectrum of restoring the surface expression of disease-associated folding-deficient SLC6 transporter variants. Thus, we have set a stage for future studies, where these data might become relevant for *in vivo* studies and generate chaperones indispensable in the clinical field.

6 References

1. Chen NH, Reith MEA, Quick MW. Synaptic uptake and beyond: the sodium- and chloride-dependent neurotransmitter transporter family SLC6. Pflüg Arch. 2004 Feb 1;447(5):519–31.

2. Kasture A, Stockner T, Freissmuth M, Sucic S. An unfolding story: Small molecules remedy misfolded monoamine transporters. Int J Biochem Cell Biol. 2017 Nov 1;92:1–5.

3. Bröer S, Gether U. The solute carrier 6 family of transporters. Br J Pharmacol. 2012 Sep;167(2):256–78.

4. Bala PA, Foster J, Carvelli L, Henry LK. SLC6 Transporters: Structure, Function, Regulation, Disease Association and Therapeutics. Mol Aspects Med. 2013 Apr;34(2–3):197–219.

5. Freissmuth M, Stockner T, Sucic S. SLC6 Transporter Folding Diseases and Pharmacochaperoning. In: Ulloa-Aguirre A, Tao YX, editors. Targeting Trafficking in Drug Development [Internet]. Cham: Springer International Publishing; 2018 [cited 2023 Oct 4]. p. 249–70. (Handbook of Experimental Pharmacology). Available from: https://doi.org/10.1007/164_2017_71

6. Bhat S, El-Kasaby A, Freissmuth M, Sucic S. Functional and Biochemical Consequences of Disease Variants in Neurotransmitter Transporters: A Special Emphasis on Folding and Trafficking Deficits. Pharmacol Ther. 2021 Jun 1;222:107785.

7. Bhat S, Hasenhuetl PS, Kasture A, El-Kasaby A, Baumann MH, Blough BE, et al. Conformational state interactions provide clues to the pharmacochaperone potential of serotonin transporter partial substrates. J Biol Chem. 2017 Oct 6;292(40):16773–86.

8. Beerepoot P, Lam VM, Salahpour A. Pharmacological Chaperones of the Dopamine Transporter Rescue Dopamine Transporter Deficiency Syndrome Mutations in Heterologous Cells. J Biol Chem. 2016 Oct 14;291(42):22053–62.

9. Colas C. Toward a Systematic Structural and Functional Annotation of Solute Carriers Transporters—Example of the SLC6 and SLC7 Families. Front Pharmacol [Internet]. 2020 [cited 2023 Oct 4];11. Available from: https://www.frontiersin.org/articles/10.3389/fphar.2020.01229

10. Liguori L, Monticelli M, Allocca M, Hay Mele B, Lukas J, Cubellis MV, et al. Pharmacological Chaperones: A Therapeutic Approach for Diseases Caused by Destabilizing Missense Mutations. Int J Mol Sci. 2020 Jan 13;21(2):489.

11. Cheng MH, Bahar I. Monoamine transporters: structure, intrinsic dynamics and allosteric regulation. Nat Struct Mol Biol. 2019 Jul;26(7):545–56.

12. Malinauskaite L, Quick M, Reinhard L, Lyons JA, Yano H, Javitch JA, et al. A mechanism for intracellular release of Na+ by neurotransmitter/sodium symporters. Nat Struct Mol Biol. 2014 Nov;21(11):1006–12.

13. Colas C, Laine E. Targeting Solute Carrier Transporters through Functional Mapping. Trends Pharmacol Sci. 2021 Jan 1;42(1):3–6.

14. Gotfryd K, Boesen T, Mortensen JS, Khelashvili G, Quick M, Terry DS, et al. X-ray structure of LeuT in an inward-facing occluded conformation reveals mechanism of substrate release. Nat Commun. 2020 Feb 21;11(1):1005.

15. Coleman JA, Green EM, Gouaux E. X-ray structures and mechanism of the human serotonin transporter. Nature. 2016 Apr;532(7599):334–9.

16. Joseph D, Pidathala S, Mallela AK, Penmatsa A. Structure and Gating Dynamics of Na+/Cl– Coupled Neurotransmitter Transporters. Front Mol Biosci [Internet]. 2019 [cited 2023 Oct 4];6. Available from: https://www.frontiersin.org/articles/10.3389/fmolb.2019.00080

17. Focht D, Neumann C, Lyons J, Eguskiza Bilbao A, Blunck R, Malinauskaite L, et al. A non-helical region in transmembrane helix 6 of hydrophobic amino acid transporter MhsT mediates substrate recognition. EMBO J. 2021 Jan 4;40(1):e105164.

18. Navratna V, Gouaux E. Insights into the mechanism and pharmacology of neurotransmitter sodium symporters. Curr Opin Struct Biol. 2019 Feb;54:161–70.

19. Forrest LR, Tavoulari S, Zhang YW, Rudnick G, Honig B. Identification of a chloride ion binding site in Na+/Cl -dependent transporters. Proc Natl Acad Sci U S A. 2007 Jul 31;104(31):12761–6.

20. Kantcheva AK, Quick M, Shi L, Winther AML, Stolzenberg S, Weinstein H, et al. Chloride binding site of neurotransmitter sodium symporters. Proc Natl Acad Sci U S A. 2013 May 21;110(21):8489–94.

21. Góral I, Łątka K, Bajda M. Structure Modeling of the Norepinephrine Transporter. Biomolecules. 2020 Jan 7;10(1):102.

22. Hussain LS, Reddy V, Maani CV. Physiology, Noradrenergic Synapse. In: StatPearls [Internet]. Treasure Island (FL): StatPearls Publishing; 2023 [cited 2023 Oct 6]. Available from: http://www.ncbi.nlm.nih.gov/books/NBK540977/

23. Tellioglu T, Robertson D. Genetic or acquired deficits in the norepinephrine transporter: current understanding of clinical implications. Expert Rev Mol Med. 2001 Nov;3(29):1–10.

24. Jha P, Ragnarsson L, Lewis RJ. Structure-Function of the High Affinity Substrate Binding Site (S1) of Human Norepinephrine Transporter. Front Pharmacol. 2020;11:217.

25. Ji W, Miao A, Liang K, Liu J, Qi Y, Zhou Y, et al. Substrate binding and inhibition mechanism of norepinephrine transporter. Nature. 2024 Sep;633(8029):473–9.

26. Pidathala S, Mallela AK, Joseph D, Penmatsa A. Structural basis of norepinephrine recognition and transport inhibition in neurotransmitter transporters. Nat Commun. 2021 Apr 13;12(1):2199.

27. Song A, Wu X. Mechanistic insights of substrate transport and inhibitor binding revealed by high-resolution structures of human norepinephrine transporter. Cell Res. 2024 Sep 2;1–4.

28. Aronson JK. “Where name and image meet”—the argument for “adrenaline”. BMJ. 2000 Feb 19;320(7233):506.

29. Zhou J. Norepinephrine transporter inhibitors and their therapeutic potential. Drugs Future. 2004 Dec;29(12):1235–44.

30. Wu D, Chen Q, Yu Z, Huang B, Zhao J, Wang Y, et al. Transport and inhibition mechanisms of human VMAT2. Nature. 2024 Feb;626(7998):427–34.

31. Camacho-Hernandez GA, Jahan K, Newman AH. Illuminating the monoamine transporters: Fluorescently labelled ligands to study dopamine, serotonin and norepinephrine transporters. Basic Clin Pharmacol Toxicol. 2022 Dec 17;

32. Robertson SD, Matthies HJG, Galli A. A closer look at amphetamine-induced reverse transport and trafficking of the dopamine and norepinephrine transporters. Mol Neurobiol. 2009 Apr;39(2):73–80.

33. Wang Z, Ordway GA, Woolverton W. Effects of cocaine on monoamine uptake as measured ex vivo. Neurosci Lett. 2007 Feb 21;413(3):191–5.

34. Sheffler ZM, Patel P, Abdijadid S. Antidepressants. In: StatPearls [Internet]. Treasure Island (FL): StatPearls Publishing; 2023 [cited 2023 Oct 22]. Available from: http://www.ncbi.nlm.nih.gov/books/NBK538182/

35. Heal DJ, Smith SL, Gosden J, Nutt DJ. Amphetamine, past and present--a pharmacological and clinical perspective. J Psychopharmacol Oxf Engl. 2013 Jun;27(6):479–96.

36. Mantle TJ, Tipton KF, Garrett NJ. Inhibition of monoamine oxidase by amphetamine and related compounds. Biochem Pharmacol. 1976 Sep 15;25(18):2073–7.

37. Grzybowski A. [The history of cocaine in medicine and its importance to the discovery of the different forms of anaesthesia]. Klin Oczna. 2007;109(1–3):101–5.

38. Abuse NI on D. National Institute on Drug Abuse. 2021 [cited 2023 Oct 15]. Cocaine DrugFacts. Available from: https://nida.nih.gov/publications/drugfacts/cocaine

39. Smith MP, Hoepping A, Johnson KM, Trzcinska M, Kozikowski AP. Dopaminergic agents for the treatment of cocaine abuse. Drug Discov Today. 1999 Jul;4(7):322–32.

40. D’Souza MS. Glutamatergic transmission in drug reward: implications for drug addiction. Front Neurosci. 2015;9:404.

41. nhs.uk [Internet]. 2021 [cited 2023 Oct 22]. Overview - Antidepressants. Available from: https://www.nhs.uk/mental-health/talking-therapies-medicine-treatments/medicines-and-psychiatry/antidepressants/overview/

42. Taylor C, Fricker AD, Devi LA, Gomes I. Mechanisms of action of antidepressants: from neurotransmitter systems to signaling pathways. Cell Signal. 2005 May;17(5):549–57.

43. Kennedy SH, Eisfeld BS. Agomelatine and its therapeutic potential in the depressed patient. Neuropsychiatr Dis Treat. 2007 Aug;3(4):423–8.

44. Gorman JM, Kent JM. SSRIs and SNRIs: broad spectrum of efficacy beyond major depression. J Clin Psychiatry. 1999;60 Suppl 4:33–8; discussion 39.

45. Kickinger S, Hellsberg E, Frølund B, Schousboe A, Ecker GF, Wellendorph P. Structural and molecular aspects of betaine-GABA transporter 1 (BGT1) and its relation to brain function. Neuropharmacology. 2019 Dec 15;161:107644.

46. Carvill GL, McMahon JM, Schneider A, Zemel M, Myers CT, Saykally J, et al. Mutations in the GABA Transporter *SLC6A1* Cause Epilepsy with Myoclonic-Atonic Seizures. Am J Hum Genet. 2015 May 7;96(5):808–15.

47. Wang J, Poliquin S, Mermer F, Eissman J, Delpire E, Wang J, et al. Endoplasmic reticulum retention and degradation of a mutation in SLC6A1 associated with epilepsy and autism. Mol Brain. 2020 May 12;13(1):76.

48. Fischer FP, Kasture AS, Hummel T, Sucic S. Molecular and Clinical Repercussions of GABA Transporter 1 Variants Gone Amiss: Links to Epilepsy and Developmental Spectrum Disorders. Front Mol Biosci [Internet]. 2022 [cited 2023 Oct 4];9. Available from: https://www.frontiersin.org/articles/10.3389/fmolb.2022.834498

49. Zafar S, Jabeen I. Structure, Function, and Modulation of γ-Aminobutyric Acid Transporter 1 (GAT1) in Neurological Disorders: A Pharmacoinformatic Prospective. Front Chem. 2018 Sep 11;6:397.

50. Nayak SR, Joseph D, Höfner G, Dakua A, Athreya A, Wanner KT, et al. Cryo-EM structure of GABA transporter 1 reveals substrate recognition and transport mechanism. Nat Struct Mol Biol. 2023 Jul;30(7):1023–32.

51. Ben-Yona A, Kanner BI. An Acidic Amino Acid Transmembrane Helix 10 Residue Conserved in the Neurotransmitter:Sodium:Symporters Is Essential for the Formation of the Extracellular Gate of the γ-Aminobutyric Acid (GABA) Transporter GAT-1 *. J Biol Chem. 2012 Mar 2;287(10):7159–68.

52. Zhang YW, Uchendu S, Leone V, Bradshaw RT, Sangwa N, Forrest LR, et al. Chloride-dependent conformational changes in the GlyT1 glycine transporter. Proc Natl Acad Sci U S A [Internet]. 2021 Mar 3 [cited 2023 Oct 4];118(10). Available from: https://www.ncbi.nlm.nih.gov/pmc/articles/PMC7958241/

53. Kanner BI. Transmembrane Domain I of the γ-Aminobutyric Acid Transporter GAT-1 Plays a Crucial Role in the Transition between Cation Leak and Transport Modes *. J Biol Chem. 2003 Feb 7;278(6):3705–12.

54. Zhu A, Huang J, Kong F, Tan J, Lei J, Yuan Y, et al. Molecular basis for substrate recognition and transport of human GABA transporter GAT1. Nat Struct Mol Biol. 2023 Jul;30(7):1012–22.

55. Rowley NM, Madsen KK, Schousboe A, Steve White H. Glutamate and GABA synthesis, release, transport and metabolism as targets for seizure control. Neurochem Int. 2012 Sep 1;61(4):546–58.

56. Jewett BE, Sharma S. Physiology, GABA. In: StatPearls [Internet]. Treasure Island (FL): StatPearls Publishing; 2024 [cited 2024 Oct 17]. Available from: http://www.ncbi.nlm.nih.gov/books/NBK513311/

57. Jin XT, Galvan A, Wichmann T, Smith Y. Localization and Function of GABA Transporters GAT-1 and GAT-3 in the Basal Ganglia. Front Syst Neurosci. 2011;5:63.

58. Knippenberg N, Bauwens M, Schijns O, Hoogland G, Florea A, Rijkers K, et al. Visualizing GABA transporters in vivo: an overview of reported radioligands and future directions. EJNMMI Res. 2023 May 12;13(1):42.

59. Sowa AR, Brooks AF, Shao X, Henderson BD, Sherman P, Arteaga J, et al. Development of Positron Emission Tomography Radiotracers for the GABA Transporter 1. ACS Chem Neurosci. 2018 Nov 21;9(11):2767–73.

60. Singh K, Kumar P, Bhatia R, Mehta V, Kumar B, Akhtar MJ. Nipecotic acid as potential lead molecule for the development of GABA uptake inhibitors; structural insights and design strategies. Eur J Med Chem. 2022 Apr 15;234:114269.

61. Kristensen AS, Andersen J, Jørgensen TN, Sørensen L, Eriksen J, Loland CJ, et al. SLC6 neurotransmitter transporters: structure, function, and regulation. Pharmacol Rev. 2011 Sep;63(3):585–640.

62. Jayaraman K, Das AK, Luethi D, Szöllősi D, Schütz GJ, Reith MEA, et al. SLC6 transporter oligomerization. J Neurochem. 2021 May;157(4):919–29.

63. Phillips BP, Gomez-Navarro N, Miller EA. Protein quality control in the endoplasmic reticulum. Curr Opin Cell Biol. 2020 Aug 1;65:96–102.

64. Asjad HMM, Nasrollahi-Shirazi S, Sucic S, Freissmuth M, Nanoff C. Relax, Cool Down and Scaffold: How to Restore Surface Expression of Folding-Deficient Mutant GPCRs and SLC6 Transporters. Int J Mol Sci. 2017 Nov 14;18(11):2416.

65. Sucic S, Kasture A, Mazhar Asjad HM, Kern C, El-Kasaby A, Freissmuth M. When transporters fail to be transported: how to rescue folding-deficient SLC6 transporters. J Neurol Neuromedicine. 2016 Dec 30;1(9):34–40.

66. Korkhov VM, Milan-Lobo L, Zuber B, Farhan H, Schmid JA, Freissmuth M, et al. Peptide-Based Interactions with Calnexin Target Misassembled Membrane Proteins into Endoplasmic Reticulum-Derived Multilamellar Bodies. J Mol Biol. 2008 Apr 25;378(2):337–52.

67. El-Kasaby A, Just H, Malle E, Stolt-Bergner PC, Sitte HH, Freissmuth M, et al. Mutations in the carboxyl-terminal SEC24 binding motif of the serotonin transporter impair folding of the transporter. J Biol Chem. 2010 Dec 10;285(50):39201–10.

68. Kozlov G, Gehring K. Calnexin cycle – structural features of the ER chaperone system. FEBS J. 2020;287(20):4322–40.

69. Antonny B, Schekman R. ER export: public transportation by the COPII coach. Curr Opin Cell Biol. 2001 Aug 1;13(4):438–43.

70. Sato K, Nakano A. Mechanisms of COPII vesicle formation and protein sorting. FEBS Lett. 2007;581(11):2076–82.

71. Li J, Soroka J, Buchner J. The Hsp90 chaperone machinery: Conformational dynamics and regulation by co-chaperones. Biochim Biophys Acta BBA - Mol Cell Res. 2012 Mar 1;1823(3):624–35.

72. Genest O, Wickner S, Doyle SM. Hsp90 and Hsp70 chaperones: Collaborators in protein remodeling. J Biol Chem. 2019 Feb 8;294(6):2109–20.

73. Schopf FH, Biebl MM, Buchner J. The HSP90 chaperone machinery. Nat Rev Mol Cell Biol. 2017 Jun;18(6):345–60.

74. Jahn M, Rehn A, Pelz B, Hellenkamp B, Richter K, Rief M, et al. The charged linker of the molecular chaperone Hsp90 modulates domain contacts and biological function. Proc Natl Acad Sci. 2014 Dec 16;111(50):17881–6.

75. Elnatan D, Betegon M, Liu Y, Ramelot T, Kennedy MA, Agard DA. Symmetry broken and rebroken during the ATP hydrolysis cycle of the mitochondrial Hsp90 TRAP1. Martin A, editor. eLife. 2017 Jul 25;6:e25235.

76. Radli M, Rüdiger SGD. Dancing with the Diva: Hsp90–Client Interactions. J Mol Biol. 2018 Sep 14;430(18, Part B):3029–40.

77. Horwich AL, Buchner J, Smock RG, Gierasch LM, Saibil HR. 3.10 Chaperones and Protein Folding. In: Egelman EH, editor. Comprehensive Biophysics [Internet]. Amsterdam: Elsevier; 2012 [cited 2023 Oct 4]. p. 212–37. Available from: https://www.sciencedirect.com/science/article/pii/B9780123749208003131

78. Lorenz OR, Freiburger L, Rutz DA, Krause M, Zierer BK, Alvira S, et al. Modulation of the Hsp90 chaperone cycle by a stringent client protein. Mol Cell. 2014 Mar 20;53(6):941–53.

79. Bukau B, Weissman J, Horwich A. Molecular Chaperones and Protein Quality Control. Cell. 2006 May 5;125(3):443–51.

80. Mayer MP, Kityk R. Insights into the molecular mechanism of allostery in Hsp70s. Front Mol Biosci. 2015 Oct 20;2:58.

81. Ben-Zvi A, De Los Rios P, Dietler G, Goloubinoff P. Active solubilization and refolding of stable protein aggregates by cooperative unfolding action of individual hsp70 chaperones. J Biol Chem. 2004 Sep 3;279(36):37298–303.

82. Morán Luengo T, Kityk R, Mayer MP, Rüdiger SGD. Hsp90 Breaks the Deadlock of the Hsp70 Chaperone System. Mol Cell. 2018 May 3;70(3):545-552.e9.

83. Genest O, Hoskins JR, Kravats AN, Doyle SM, Wickner S. Hsp70 and Hsp90 of E. coli directly interact for collaboration in protein remodeling. J Mol Biol. 2015 Dec 4;427(24):3877–89.

84. Doyle SM, Hoskins JR, Kravats AN, Heffner AL, Garikapati S, Wickner S. Intermolecular interactions between Hsp90 and Hsp70. J Mol Biol. 2019 Jul 12;431(15):2729–46.

85. Hoter A, El-Sabban ME, Naim HY. The HSP90 Family: Structure, Regulation, Function, and Implications in Health and Disease. Int J Mol Sci. 2018 Aug 29;19(9):2560.

86. Gupta A, Bansal A, Hashimoto-Torii K. HSP70 and HSP90 in neurodegenerative diseases. Neurosci Lett. 2020 Jan 18;716:134678.

87. Lackie RE, Maciejewski A, Ostapchenko VG, Marques-Lopes J, Choy WY, Duennwald ML, et al. The Hsp70/Hsp90 Chaperone Machinery in Neurodegenerative Diseases. Front Neurosci [Internet]. 2017 [cited 2023 Oct 29];11. Available from: https://www.frontiersin.org/articles/10.3389/fnins.2017.00254

88. Wacker JL, Zareie MH, Fong H, Sarikaya M, Muchowski PJ. Hsp70 and Hsp40 attenuate formation of spherical and annular polyglutamine oligomers by partitioning monomer. Nat Struct Mol Biol. 2004 Dec;11(12):1215–22.

89. Li ZN, Luo Y. HSP90 inhibitors and cancer: Prospects for use in targeted therapies (Review). Oncol Rep. 2023 Jan;49(1):6.

90. Ambrose AJ, Chapman E. Function, Therapeutic Potential, and Inhibition of Hsp70 Chaperones. J Med Chem. 2021 Jun 10;64(11):7060–82.

91. Brüss M, Kunz J, Lingen B, Bönisch H. Chromosomal mapping of the human gene for the tricyclic antidepressant-sensitive noradrenaline transporter. Hum Genet. 1993 Apr;91(3):278–80.

92. Moroz MA, Serganova I, Zanzonico P, Ageyeva L, Beresten T, Dyomina E, et al. Imaging hNET reporter gene expression with 124I-MIBG. J Nucl Med Off Publ Soc Nucl Med. 2007 May;48(5):827–36.

93. Hahn MK, Mazei-Robison MS, Blakely RD. Single nucleotide polymorphisms in the human norepinephrine transporter gene affect expression, trafficking, antidepressant interaction, and protein kinase C regulation. Mol Pharmacol. 2005 Aug;68(2):457–66.

94. Hahn MK, Robertson D, Blakely RD. A Mutation in the Human Norepinephrine Transporter Gene (SLC6A2) Associated with Orthostatic Intolerance Disrupts Surface Expression of Mutant and Wild-Type Transporters. J Neurosci. 2003 Jun 1;23(11):4470–8.

95. Sengupta SM, Grizenko N, Thakur GA, Bellingham J, DeGuzman R, Robinson S, et al. Differential association between the norepinephrine transporter gene and ADHD: role of sex and subtype. J Psychiatry Neurosci JPN. 2012 Mar;37(2):129–37.

96. Chiba P, Freissmuth M, Stockner T. Defining the blanks – Pharmacochaperoning of SLC6 transporters and ABC transporters. Pharmacol Res. 2014 May;83(100):63–73.

97. Shannon JR, Flattem NL, Jordan J, Jacob G, Black BK, Biaggioni I, et al. Orthostatic Intolerance and Tachycardia Associated with Norepinephrine-Transporter Deficiency. N Engl J Med. 2000 Feb 24;342(8):541–9.

98. Hahn MK, Steele A, Couch RS, Stein MA, Krueger JJ. Novel and functional norepinephrine transporter protein variants identified in attention-deficit hyperactivity disorder. Neuropharmacology. 2009 Dec;57(7–8):694–701.

99. Choo M, Hwang JA, Jeon SW, Oh SY, Yoon HK, Lee HJ, et al. Association Study between Norepinephrine Transporter Gene Polymorphism and Schizophrenia in a Korean Population. Psychiatry Investig. 2015 Oct;12(4):551–8.

100. Fichna JP, Humińska-Lisowska K, Safranow K, Adamczyk JG, Cięszczyk P, Żekanowski C, et al. Rare Variant in the SLC6A2 Encoding a Norepinephrine Transporter Is Associated with Elite Athletic Performance in the Polish Population. Genes. 2021 Jun 15;12(6):919.

101. Piniella D, Canseco A, Vidal S, Xiol C, Díaz de Bustamante A, Martí-Carrera I, et al. Experimental and Bioinformatic Insights into the Effects of Epileptogenic Variants on the Function and Trafficking of the GABA Transporter GAT-1. Int J Mol Sci. 2023 Jan 4;24(2):955.

102. Devries S, Mulder M, Charron JG, Prokop JW, Mark PR. SLC6A1 G443D associated with developmental delay and epilepsy. Cold Spring Harb Mol Case Stud. 2020 Aug;6(4):a005371.

103. Cai K, Wang J, Eissman J, Wang J, Nwosu G, Shen W, et al. A missense mutation in *SLC6A1* associated with Lennox-Gastaut syndrome impairs GABA transporter 1 protein trafficking and function. Exp Neurol. 2019 Oct 1;320:112973.

104. Sato S, Ward CL, Krouse ME, Wine JJ, Kopito RR. Glycerol reverses the misfolding phenotype of the most common cystic fibrosis mutation. J Biol Chem. 1996 Jan 12;271(2):635–8.

105. Tao YX, Conn PM. Pharmacoperones as Novel Therapeutics for Diverse Protein Conformational Diseases. Physiol Rev. 2018 Apr 1;98(2):697–725.

106. Perlmutter DH. Chemical Chaperones: A Pharmacological Strategy for Disorders of Protein Folding and Trafficking. Pediatr Res. 2002 Dec;52(6):832–6.

107. El-Kasaby A, Kasture A, Koban F, Hotka M, Asjad HMM, Kubista H, et al. Rescue by 4-phenylbutyrate of several misfolded creatine transporter-1 variants linked to the creatine transporter deficiency syndrome. Neuropharmacology. 2019 Dec 15;161:107572.

108. Stein D, Slobodnik Z, Tam B, Einav M, Akabayov B, Berstein S, et al. 4-phenylbutyric acid—Identity crisis; can it act as a translation inhibitor? Aging Cell. 2022;21(12):e13738.

109. Shah N, Kasture AS, Fischer FP, Hummel T, Sucic S. A transporter´s doom or destiny: SLC6A1 in health and disease, novel molecular targets and emerging therapeutic prospects. Front Mol Neurosci [Internet]. 2024 Aug 29 [cited 2024 Oct 8];17. Available from: https://www.frontiersin.org/journals/molecular-neuroscience/articles/10.3389/fnmol.2024.1466694/full

110. Bhat S, Guthrie DA, Kasture A, El-Kasaby A, Cao J, Bonifazi A, et al. Tropane-Based Ibogaine Analog Rescues Folding-Deficient Serotonin and Dopamine Transporters. ACS Pharmacol Transl Sci. 2020 Aug 28;4(2):503–16.

111. Kim JG, Lee SC, Kim OH, Kim KH, Song KY, Lee SK, et al. HSP90 inhibitor 17-DMAG exerts anticancer effects against gastric cancer cells principally by altering oxidant-antioxidant balance. Oncotarget. 2017 Apr 10;8(34):56473–89.

112. Kasture AS, Fischer FP, Kunert L, Burger ML, Burgstaller AC, El-Kasaby A, et al. Drosophila melanogaster as a model for unraveling unique molecular features of epilepsy elicited by human GABA transporter 1 variants. Front Neurosci [Internet]. 2023 Jan 19 [cited 2024 Dec 12];16. Available from: https://www.frontiersin.org/journals/neuroscience/articles/10.3389/fnins.2022.1074427/full

113. Wainwright CE, Elborn JS, Ramsey BW, Marigowda G, Huang X, Cipolli M, et al. The New England Journal of Medicine. Massachusetts Medical Society; 2015 [cited 2025 Jan 20]. Lumacaftor–Ivacaftor in Patients with Cystic Fibrosis Homozygous for Phe508del CFTR. Available from: https://www.nejm.org/doi/full/10.1056/NEJMoa1409547

List of Figures

List of Tables

Abbreviations

4-PBA: 4-phenylbutyric acid

17-DMAG: 17-dimethylaminoethylamino-17-demethoxygeldanamycin

ADHD: Attention Deficit Hyperactivity Disorder

ALS: Amyotrophic Lateral Sclerosis

ANOVA: Analysis of Variance

ATP: Adenosine Triphosphate

BBB: Blood Brain Barrier

BGT: Betaine-GABA-Transporter

CNS: Central Nervous System

CTD: C-Terminal Domain

CFP-CNX: Cyan-Fluorescent-Protein-Calnexin

CFTR: Cystic Fibrosis Transmembrane Conductance Regulator

COP: Coat Protein Complex

CRT: Creatine Transporter

DA: Dopamine

DAT: Dopamine Transporter

DHPG: Dihydroxyphenylglycol

DMEM: Dulbecco's Modified Eagle Medium

DMSO: Dimethyl sulfoxide

EDTA: Ethylenediaminetetraacetic Acid

EEVD: Glutamic Acid-Glutamic acid-Valine-Aspartic acid

EL: Extracellular Loop

ER: Endoplasmic Reticulum

ERAD: Endoplasmic-Reticulum-Associated-Degradation

ERGIC: ER–Golgi Intermediate Compartment

GABA: γ -Amino-Butyric Acid

GAT: GABA Transporter

HEK293 cells: Human Embryonic Kidney 293 cells

HSP: Heat Shock Protein

IL: Intracellular Loop

LA: Lipophectamine

MAE: Myoclonic Atonic Epilepsy

MAO: Monoaminooxidase

MAOI: MAO Inhibitor

MAT: Monoamino Transporter

MEEVD: Methionine-Glutamic Acid-Glutamic acid-Valine-Aspartic acid

MD: Middle domain

NASSA: Norepinephrine and Specific Serotonergic Antidepressants

NBD: Nucleotide-Binding-Domain

NE/NA: Norepinephrine/Noradrenaline

NEF: Nucleotide-Exchange Factor

NET: NE Transporter

NTD: N-Terminal Domain

NSS: Neurotransmitter-Sodium-Symporter

PBS: Phosphate Buffered Saline

PVDF: Polyvinylidene Difluoride

SBD: Substrate-Binding-Domain

SDS-PAGE: Sodium Dodecyl Sulfate Polyacrylamide Gel Electrophoresis

SERT: Serotonin Transporter

SLC: Solute Carrier

SNP: Single Nucleotide Polymorphism

siRNA: small interfering RNA

SSRI: Selective Serotonin Reuptake Inhibitor

TBST: Tris-buffered saline containing 0.1% Tween 20

TCA: Tricyclic Antidepressant

TM: Transmembrane Domain

UGGT: UDP-glucose-glycoprotein glucosyltransferase

$VMAT_2$: Vesicular Monoamine Transporter 2

YFP: Yellow-Fluorescent-Protein

Molecular Structures

Tyrosine

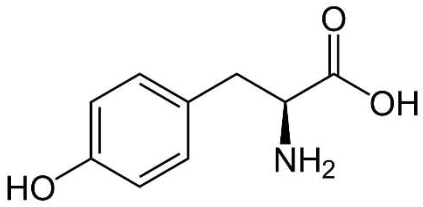

L-DOPA

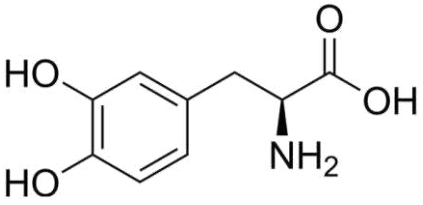

Dopamine

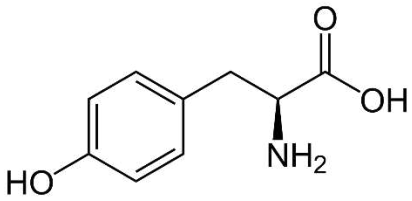

Norepinephrine

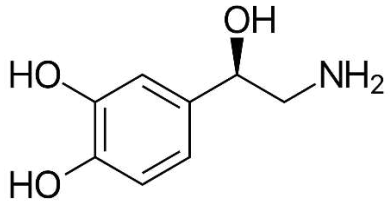

Glutamate

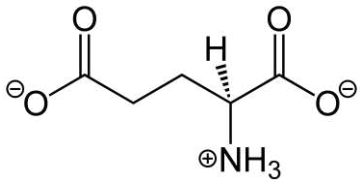

Glutamine

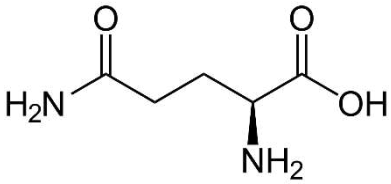

GABA

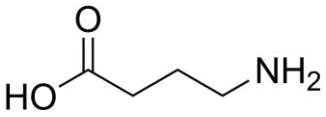

α-Ketoglutaric acid

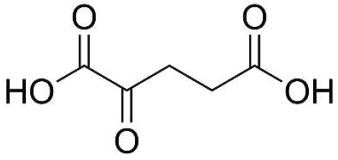

Succinic semialdehyde

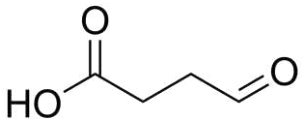

Succinate

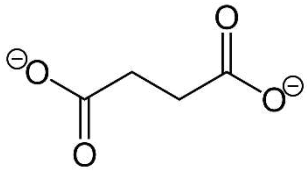

Nipecotic acid

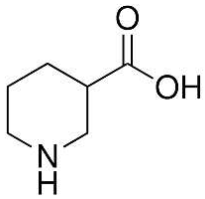

Tiagabine

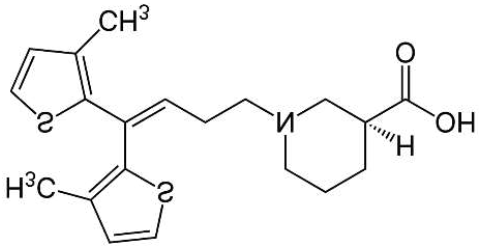

Guvacine

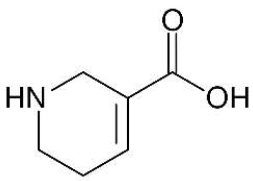

Glycerol

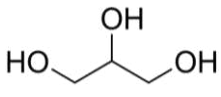

DMSO

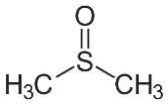

4-PBA

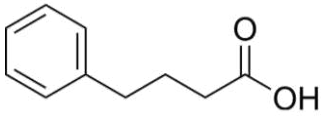

Pifithrin-μ

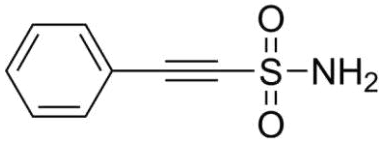

17-DMAG

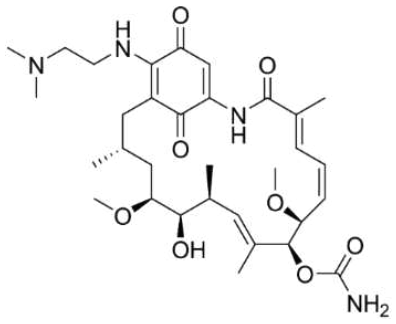

Noribogaine

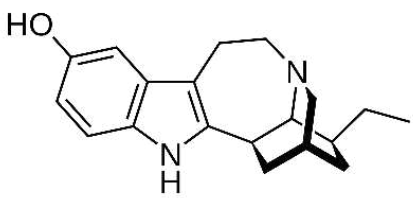

Bupropion

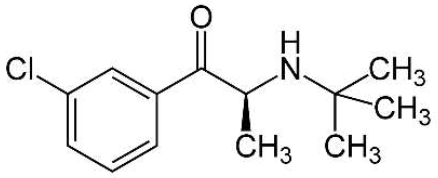

Tiagabine

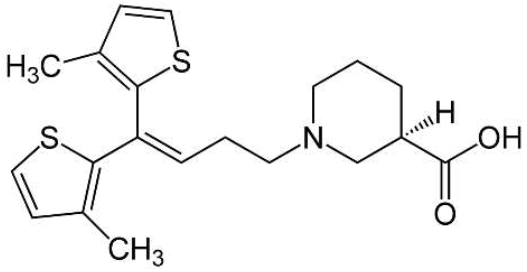

Lumacaftor

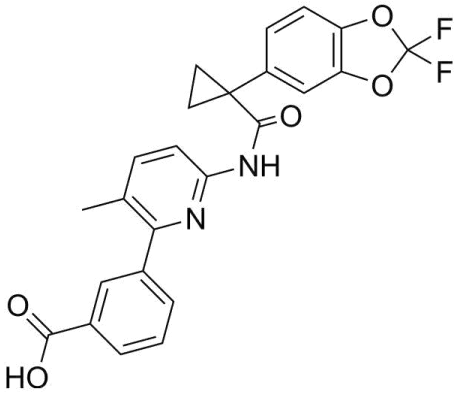

Migalastat

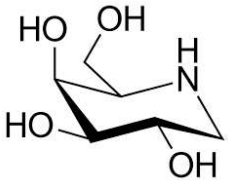

Tafamidis